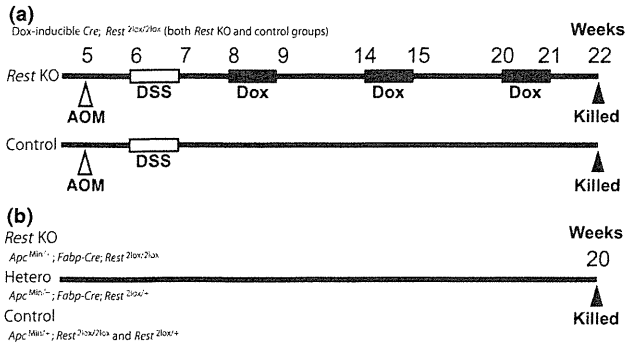

Fig. 1. Schematic drawing of the experimental protocols. The two experiments are different in terms of the timing of the *Rest* recombination. (a) Protocol 1 (*Rest* ablation at the post-initiation phase). (b) Protocol 2 (*Rest* ablation at the pre-initiation phase). Black arrowheads, mice killed; black bars, doxycycline (Dox); white arrowheads, azoxymethane (AOM); white bars, dextran sodium sulfate (DSS). KO, knockout.

Cre-mediated genetic recombination in the intestinal epithelia started before the completion of intestinal morphogenesis, thereby mimicking when the *Rest* recombination occurs before the initiation of carcinogenesis.

In protocol 1, doxycycline-inducible *Cre*; $Rest^{2lox/2lox}$ mice were separated into a *Rest* KO group (n = 27) and a control group (n = 11). Five-week-old mice were given a single i.p. injection of azoxymethane (15 mg/kg body weight; Wako, Osaka, Japan), a colon-specific carcinogen. One week later, the mice were fed dextran sodium sulfate (20 mg/mL; Wako), a potent tumor promoter for colon tumorigenesis, in their drinking water for 1 week. The mice in the *Rest* KO group were fed 2 mg/mL doxycycline (Sigma, St. Louis, MO, USA) in their drinking water, supplemented with 10 mg/mL sucrose three times per week (at weeks 8, 14, and 20), whereas mice in the control group were fed tap water throughout the experiment. All mice were killed at 22 weeks of age.

In protocol 2, intestine-specific *Rest* KO mice ($Apc^{Min/+}$; *Fabp-Cre*$^{+}$; $Rest^{2lox/2lox}$ mice, n = 23), heterozygous *Rest* KO mice ($Apc^{Min/+}$; *Fabp-Cre*$^{+}$; $Rest^{2lox/+}$ mice, n = 32), and control mice ($Apc^{Min/+}$; *Fabp-Cre*$^{-}$; $Rest^{2lox/2lox}$ mice and $Apc^{Min/+}$; *Fabp-Cre*$^{-}$; $Rest^{2lox/+}$ mice, n = 26) were examined for the development of colon tumors. All mice were housed in rooms without any chemical treatment during the experiment and were killed at 20 weeks of age.

In both protocols, the colons were cut open longitudinally, then washed with PBS. Visible tumors (larger than 0.5 mm in their maximum diameters) on the colon mucosa were counted, and their maximum diameters were measured. Tumor samples were fixed in 10% buffered formalin for 24 h and embedded in paraffin. Sections were stained with H&E, then serial sections were used for the immunohistochemical analysis. Immunostaining was carried out using an avidin–biotin immunoperoxidase assay. The primary antibodies used in the immunostaining were anti-β-catenin (1:1000 dilution; BD Biosciences, San Diego, CA, USA), anti-chromogranin A (1:1000 dilution; Dako, Carpinteria, CA, USA), and anti-Ki-67 (1:100 dilution; Dako).

Crypt isolation. In order to examine the effect of *Rest* ablation in the colonic epithelium, we carried out crypt isolation to exclude the contaminating stromal cells in the colonic mucosa, as described previously.[29] The removed colon was cut into three equal segments. The distal segment was used for crypt isolation.

Confirmation of *Rest* recombination. To examine the recombination status of the conditional *Rest* allele in the colon, we carried out a Southern blot analysis of the *Rest* loci. Total DNA was extracted from isolated intestinal crypts of doxycycline-inducible *Rest* knockout mice at the indicated time intervals (Fig. 2a). DNA samples (10 μg each) were digested with Mfe1 (Bio-Rad, Hercules, CA, USA). The digested DNA samples were electrophoresed, transferred onto nylon membranes, and hybridized with a DIG probe against the *Rest* loci in PerfectHyb (Toyobo, Osaka, Japan).[26] Signals were detected by chemiluminescence with LAS-4000 (Fujifilm, Tokyo, Japan). We also carried out a PCR-based analysis to examine the recombination of the *Rest* gene in colon tumors. DNA was isolated from formalin-fixed paraffin-embedding blocks using the Pinpoint Slide DNA Isolation System (Zymo Research, Orange, CA, USA). The PCR was carried out using primers specific for mouse floxed *Rest*. The primers for the $Rest^{2lox}$ allele were forward (F) (5′-CCCTTATGGGTGCAAGTGTT-3′) and reverse (R) (5′-GGGGGACAAAGCCACTCTA-3′). The primers for $Rest^{1lox}$ allele were F (5′-GGGTGCAAGTGTTCTCTTGTCT-3′) and R (5′-CAAGTAACTAAAAATTAGGAACTACCG-3′).

Real-time PCR analysis. Total RNA was extracted from the isolated intestinal crypts as described previously (Fig. 2a), and from the colon tumors of $Apc^{Min/+}$ mice using the RNeasy Mini kit (Qiagen, Valencia, CA, USA). Total RNA (0.5 μg each) was reverse transcribed using Superscript III Reverse Transcriptase (Invitrogen, Carlsbad, CA, USA).

Quantitative real-time PCR was carried out with the Thermal Cycler Dice Real Time System Single (Takara, Kyoto, Japan) using the SYBR Green (Takara) method. The primer sequences used in the quantitative real-time PCR analyses for *Bdnf*, *Tubb3*, and *Rest* were obtained from PrimerBank (http://pga.mgh.harvard.edu/primerbank/). The primers for β-*actin* were F (5′-CATCCGTAAAGACCTCTATGCCAAC-3′) and R (5′-ATGGAGCCACCGATCCACA-3′). The primers for *Gfp* were F (5′-ACCAGCAGAACACCCCCATC-3′) and R (5′-AGCTCGTCCATGCCGAGAGT-3′). The primers for *Syt4* were F (5′-TGCTTTTGGCCTCGTCTTCA-3′) and R (5′-GCGGTTTTACCCTTCACTTCAC-3′).

Statistical analysis. Statistical significance was evaluated using either Student's t-test or Welch's t-test for paired samples. The results of experiments are presented as the mean ± SEM. $P < 0.05$ was considered to indicate a significant difference.

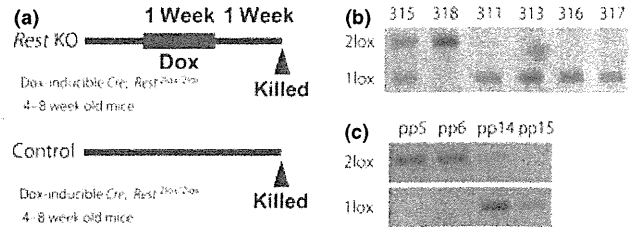

Fig. 2. Genetic recombination of the *Rest* alleles. (a) Doxycycline (Dox)-mediated recombination of *Rest* in protocol 1. A schematic drawing of the experiment. *Rest* conditional knockout (KO) mice with Dox-inducible *Cre* alleles at 4–8 weeks old were treated with 0.2% Dox in their drinking water for 1 week (black bar). Black arrowheads, mice killed. (b) In the Southern blot analysis, in contrast to the control crypts (non-Dox-treated crypts; 315, 318), most of the 2lox alleles in the Dox-treated colonic crypts (311, 313, 316, 317) recombined into 1lox KO alleles. In some cases, the control crypts also contained 1lox alleles (315), probably due to the leaky expression of the *Cre* recombinase. (c) *Rest* recombination in colon tumors in protocol 2. We carried out a PCR-based analysis for *Rest* recombination using colon tumor sections in protocol 2. We could confirm the 1lox KO alleles in five out of six tumors in the *Rest* conditional KO mice with the *Fabp-Cre* allele (pp14 and pp15). However, no recombined *Rest* alleles were observed in any of the nine tumors examined from control mice without the *Fabp-Cre* allele (pp5 and pp6).

doi: 10.1111/j.1349-7006.2011.02006.x

Results

***Cre* expression induces genetic ablation of *Rest* in colonic mucosa.** In order to examine the efficiency of *Rest* recombination in protocol 1, we carried out a Southern blot analysis using genomic DNA from isolated colonic crypts of doxycycline-inducible *Cre*; $Rest^{2lox/2lox}$ mice (Fig. 2a). The Southern blot analysis revealed that the majority of the $Rest^{2lox}$ alleles in the colonic crypts were recombined into $Rest^{1lox}$ alleles in doxycycline-treated mice (the $Rest^{1lox}$ allele was confirmed in seven out of eight colonic crypts). However, partial recombination of the *Rest* allele was also observed in some cases in the non-treated group (5 out of 13 colonic crypts), probably due to the leaky expression of the *Cre* transgene (Fig. 2b).

In protocol 2, *Rest* recombination was examined using a PCR assay with genomic DNA from formalin-fixed paraffin-embedding specimens of *Fabp-Cre*$^{+}$; $Rest^{2lox/2lox}$ mice. The recombined *Rest* gene ($Rest^{1lox}$ allele) was only detected in mice containing the *Fabp-Cre* allele, and the $Rest^{2lox}$ allele was also detected in these mice, indicating partial recombination, which is consistent with a previous experiment showing a recombination efficiency of approximately 50% in the colonic crypts by the *Fabp-Cre* allele (Fig. 2c).[28] These results indicate that genetic ablation of *Rest* was induced successfully in the colons of two independent *Cre*-expressing mouse models. In both protocol 1 and 2, despite the presence of the $Rest^{1lox}$ allele, the mice were healthy, and no detectable difference was observed in the histological analyses in comparison to the control mice.

Transcript levels of *Rest* and Rest-targeted genes in colonic mucosa. We next examined the expression levels of *Rest* in colonic tumors of $Apc^{Min/+}$ mice. The quantitative real-time PCR analysis revealed that *Rest* expression is not different between the colon tumors and non-neoplastic normal mucosa, suggesting that loss of *Rest* is not involved in the colon tumorigenesis of $Apc^{Min/+}$ mice (Fig. 3a). In order to elucidate the effect of genetic ablation of *Rest* in the colonic mucosa, we measured the mRNA expression levels of the *Rest* gene and Rest-targeted genes in the isolated colonic crypts of doxycycline-inducible *Cre*; $Rest^{2lox/2lox}$ mice by quantitative real-time PCR analysis (Fig. 2a). Consistent with the genetic recombination observed in the Southern blot analysis, the expression of *Rest* in the colonic crypts was significantly decreased in the doxycycline-treated mice in comparison with the non-treated mice (Fig. 3b). In line with the decreased expression of the *Rest* gene, the expression of *Gfp* was also downregulated in the doxycycline-treated crypts (Fig. 3c). In contrast, the expression of *Syt4*, *Bdnf*, and *Tubb3*, which are known to be Rest-targeted genes, were significantly upregulated in the doxycycline-treated crypts (Fig. 3d). These results indicate that the genetic recombination of *Rest* results in the rapid derepression of the Rest-targeted genes, suggesting that *Rest* plays a role in the repression of neuronal genes in the colonic crypts.

Macroscopic analysis of colon tumor development. Macroscopically, polypoid tumors were observed in colonic mucosa of mice during both experiments. In protocol 1, genetic recombination into the $Rest^{1lox}$ allele was only confirmed in *Cre*-induced tumors ($n = 4$). In protocol 2, the recombined *Rest* allele ($Rest^{1lox}$ allele) was detectable in the majority of *Rest* KO tumors (5 out of 6 tumors), whereas all control tumors ($n = 9$) retained non-recombined *Rest* alleles ($Rest^{2lox/2lox}$) (Fig. 2c). In protocol 1, the multiplicity of colon tumors was 0.37 ± 0.14/mouse in the *Rest* KO mice and 0.18 ± 0.18/mouse in control mice (Fig. 4a). In protocol 2, the multiplicity and the maximum diameter of colon tumors were 4.96 ± 0.57/mouse and 3.31 ± 0.12 mm in the *Rest* KO mice, 4.81 ± 0.51/mouse and 3.37 ± 0.12 mm in the *Rest* heterozygous mice, and 4.35 ± 0.71/mouse and 3.68 ± 0.15 mm in the control mice, respectively (Fig. 4b,c). No macroscopic tumors were observed

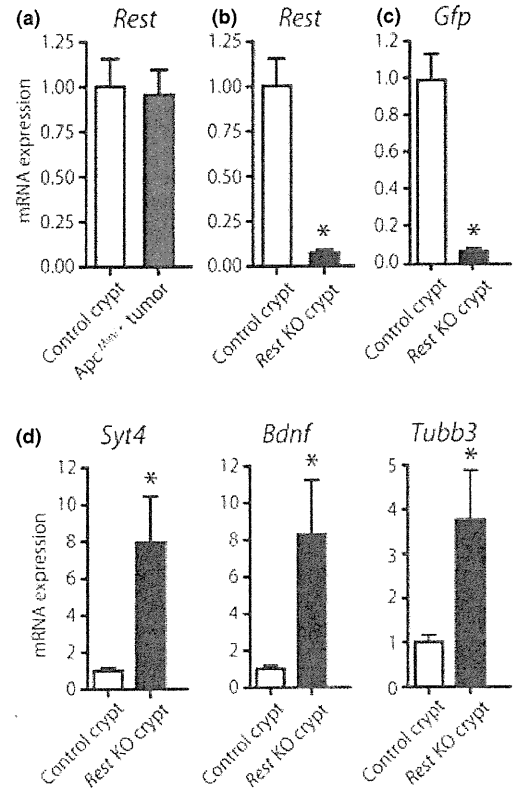

Fig. 3. Transcriptional levels of *Rest* and Rest-targeted neuronal genes in the colon mucosa. (a) $Apc^{Min/+}$ colonic tumors with wild-type *Rest* alleles had nearly the same *Rest* expression level as non-neoplastic crypts. (b–d) Expression levels of *Rest* (b) and *Gfp* (c) were downregulated after the *Rest* ablation in colonic crypts, whereas the expression levels of the Rest-targeted genes (d), *Syt4*, *Bdnf*, and *Tubb3* were significantly upregulated. The mRNA expression levels were analyzed by quantitative real-time PCR and were normalized to the β-actin levels. Data are presented as the mean ± SEM of 13 independent samples. $*P < 0.05$.

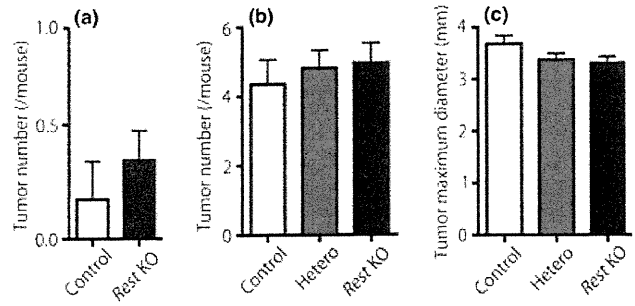

Fig. 4. Macroscopic analysis of colon tumor development. (a) The number of macroscopic tumors in protocol 1. (b,c) The number of macroscopic tumors (b) and the size of tumors (c) in protocol 2. Data are presented as the mean ± SEM.

in the intestine-specific *Rest* KO mice without the Apc^{Min} allele ($Apc^{+/+}$; *Fabp-Cre*$^{+}$; $Rest^{2lox/2lox}$ mice, $n = 4$). Furthermore, a lack of colon tumor development in *Fabp-Cre*$^{+}$; $Rest^{2lox/2lox}$ mice was also confirmed in the mice older than 12 months (data not shown), thus suggesting that *Rest* ablation alone is not sufficient to initiate colon tumorigenesis.

Collectively, the multiplicity of colon tumors in the *Rest* KO mice was slightly higher than that in the control mice, but the difference between the *Rest* KO and control mice was not

significantly different (protocol 1: *Rest* KO *vs.* control, $P = 0.46$; protocol 2: *Rest* KO *vs.* control, $P = 0.51$). In addition, no statistically significant difference was observed in the size of the colon tumors, although there was a tendency for the tumor size to correlate with the expression of *Rest* (protocol 2: *Rest* KO *vs.* control, $P = 0.054$).

Histological and immunohistochemical analyses of colon tumors. Colon tumors were processed for histological examinations. As *Rest* recombination occurs partially by the *Fabp-Cre* transgene in protocol 2, the genetic status of *Rest* was determined in each tumor by PCR using primers specific for the $Rest^{2lox}$ and $Rest^{1lox}$ alleles. Regardless of the *Rest* recombination, the histological analysis revealed that all colon tumors consisted of tubular dysplastic glands. There were no detectable histological differences between the colon tumors of *Rest* KO and control mice in either protocol (Fig. 5a).

We further analyzed these tumors by immunostaining for β-catenin, Ki-67, and chromogranin A. The accumulation of β-catenin protein is a critical event that occurs during colon carcinogenesis. Indeed, in the present study, the accumulation of β-catenin was observed in the dysplastic glands in the colonic tumors. However, the β-catenin immunostaining showed no detectable difference between colon tumors in the *Rest* KO and control mice in either protocol (Fig. 5a).

We also carried out Ki-67 immunostaining to compare the proliferative activities of tumor cells with different genetic status of *Rest*. We counted Ki-67 immunopositive tumor cells out of 1000 randomly selected colonic tumor cells from *Rest* KO and control mice, and calculated the ratio of Ki-67 positive tumor cells. The Ki-67 positive cell ratios in the colon tumors of *Rest* KO and control mice were $27.6 \pm 3.39\%$ ($n = 5$) and $31.4 \pm 4.84\%$ ($n = 5$) in protocol 1 ($P = 0.53$), and $44.2 \pm 3.00\%$ ($n = 10$) and $41.2 \pm 2.53\%$ ($n = 11$) in protocol 2 ($P = 0.45$), respectively (Table 1).

Rest has been shown to be a master negative regulator of neuronal differentiation. Indeed, we confirmed that genetic ablation of *Rest* leads to the derepression of neuronal gene expression. Therefore, we next examined the enteroendocrine cell differentiation of the intestinal cells after loss of *Rest* expression. Chromogranin A immunostaining was used to assess the endocrine differentiation of both non-neoplastic and tumor cells in the colon. Chromogranin A immunostaining showed no detectable differences related to the *Rest* recombination in both non-neoplastic and tumor cells (Fig. 5b). The positive cell ratios for chromogranin A in *Rest* KO and control tumors was $0.28 \pm 0.08\%$ ($n = 5$) and $0.10 \pm 0.07\%$ ($n = 5$) in protocol 1 ($P = 0.12$), and $0.07 \pm 0.02\%$ ($n = 10$) and $0.12 \pm 0.02\%$ ($n = 11$) in protocol 2 ($P = 0.17$), respectively (Table 1).

Discussion

Colon carcinogenesis is a multistage process involving genetic and epigenetic alterations of various tumor suppressor genes and oncogenes. Our previous studies identified two distinct stages of colon tumorigenesis in $Apc^{Min/+}$ mice (microadenomas and macroscopic tumors).[30] The formation of microadenomas is accompanied by the activation of the canonical Wnt pathway through the genetic loss of the *Apc* gene, leading to the accumulation of β-catenin. Recent evidence suggests that DNA methylation is closely associated with the progression of microadenomas into macroscopic tumors.[28,31–33] Although the identity of the target genes of DNA methylation involved in colon tumorigenesis remain unclear, these findings suggest that the progression of colonic tumors in $Apc^{Min/+}$ mice requires synchronous alternations in the expression of multiple genes due to global changes of epigenetic modifications.

REST, a novel candidate tumor suppressor gene in colon carcinogenesis, maintains transcriptional silencing of various genes by recruiting multiple co-factors, including Co-Rest,[27] HDAC and Sin3 complex,[34–36] histone H3 K9 methyltransferase G9a,[37] histone H3 K4 demethylase LSD1,[38] and methyl DNA binding protein MeCP2.[39] Previous experiments indicated

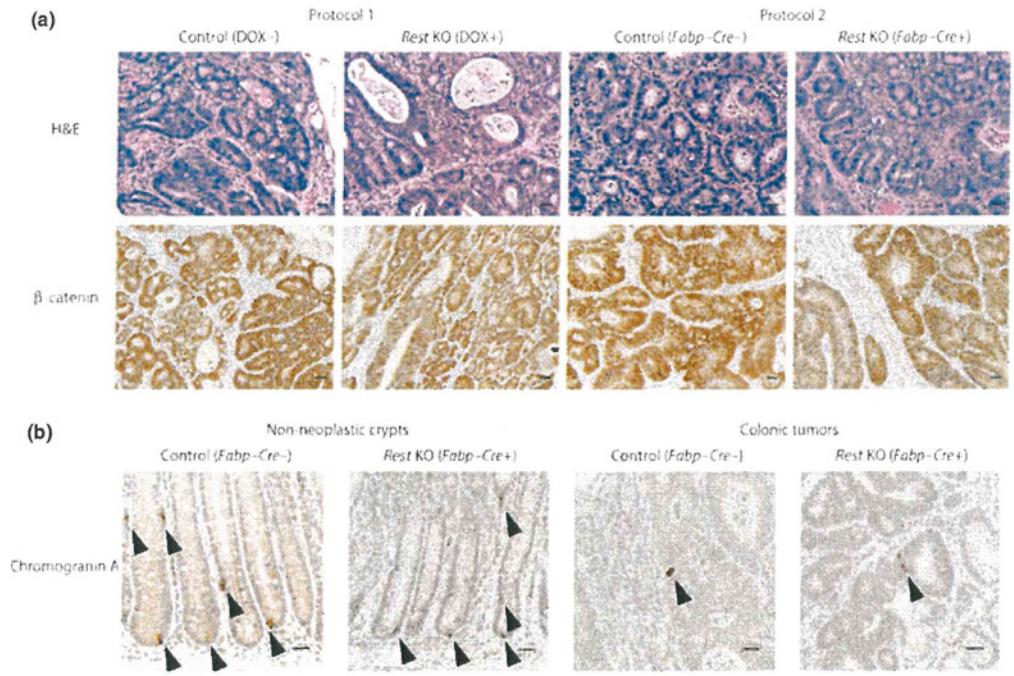

Fig. 5. Histological and immunohistochemical analyses of colonic tumors. (a) There was no detectable difference in the H&E staining (upper panels) and β-catenin immunostaining (lower panels) between the *Rest* knockout (KO) and control tumors in either protocol. (b) Chromogranin A immunostaining of colonic non-neoplastic and tumor cells. Black arrowheads, chromogranin A immunopositive cells, *Rest* KO: $Apc^{Min/+}$; *Fabp-Cre*$^{+}$; $Rest^{2lox/2lox}$ mice, control: $Apc^{Min/+}$; $Rest^{2lox/2lox}$ mice. Dox, doxycycline. Scale bars = 20 μm.

doi: 10.1111/j.1349-7006.2011.02006.x

Table 1. Ki-67 and chromogranin A positive tumor cell ratio in colon tumors of *Rest* knockout (KO) and control mice

		Ki-67 (%)	Chromogranin A (%)
Protocol 1	*Rest* KO	27.6 ± 3.39	0.28 ± 0.08
	Control	31.4 ± 4.84	0.10 ± 0.07
Protocol 2	*Rest* KO	44.2 ± 3.00	0.07 ± 0.02
	Control	41.2 ± 2.53	0.12 ± 0.02

Protocol 1, chemically-induced colon carcinogenesis model using doxycycline-inducible *Cre*-expressing mice. Protocol 2, $Apc^{Min/+}$ mouse colon carcinogenesis model combined with *Fabp-Cre* mouse.

thousands of REST-targeted genes in embryonic stem cells and neuronal progenitor cells.[40] REST is thus suggested to alter the chromatin structure in conjunction with its co-factors, while also regulating the transcription of the REST-targeted genes through histone modification, chromatin remodeling, and genomic methylation. Given the fact that DNA methylation, one of the most important epigenetic modifications, plays a critical role in the transition from microadenomas to macroscopic tumors in the colon of $Apc^{Min/+}$ mice, we hypothesized that the global changes in epigenetic modifications caused by *Rest* ablation might affect murine colon tumorigenesis.

In this study, we confirmed that the genetic ablation of *Rest* leads to the decreased expression of *Rest* and increased expression of Rest-targeted genes, suggesting that Rest represses the Rest-targeted genes in the colonic crypts. However, *Rest* ablation at both the pre-initiation and post-initiation phases of colon tumorigenesis showed no significant effect on tumor development in the colon. These findings indicate that loss of *Rest* expression by itself does not promote the development of colon tumors in mice. It is possible that *Rest* deletion alone might not be sufficient for the active changes of epigenetic modifications to induce the progression of colon tumorigenesis.

Rest has been regarded as a master negative regulator of neuronal differentiation in non-neuronal cells. Indeed, a targeted mutation of *Rest* in mice caused derepression of neuron-specific genes in a subset of non-neuronal tissues. Human colonic carcinoma expressing neuroendocrine genes (also called neuroendocrine carcinoma, NEC) is a highly aggressive carcinoma that comprises approximately 0.6% of colonic carcinomas.[41] Importantly, most neuroendocrine genes expressed in NEC are targets of the REST-repressing complex. Considering that the genetic deletion of *Rest* leads to the upregulation of neuronal genes in non-neuronal cells, we hypothesized that *Rest* deletion would induce neuronal differentiation in colonic tumors, thus leading to a NEC-like phenotype. In fact, previous studies have revealed that carcinomas with *REST* dysfunction frequently showed neuroendocrine characteristics.[8,12–16] However, in the present study, colon tumors lacking the *Rest* gene did not show the NEC-like histology. In addition, an increase in chromogranin A-positive cells, which is usually observed in NEC, was not detectable in the *Rest*-deleted tumors. Our results suggest that, although *Rest* ablation leads to the increased mRNA expression of neuronal genes, *Rest* ablation alone is not sufficient to induce neuronal differentiation in the colon. As the incidence of NEC is extremely rare compared to the relatively high incidence of *REST* deletion in colorectal cancer,[24,41] it is still possible that *REST* inactivation, in conjunction with additional genetic and/or epigenetic alterations, may be involved in the development of NEC. In this context, it would be interesting to examine the genetic status of *REST* in NEC in future studies.

In summary, we have shown that the genetic ablation of *Rest* does not affect the development of colon tumors in mice. These findings suggest that other genetic and/or epigenetic alterations might therefore be required to exert the tumor-promoting effect of *Rest* ablation during multistage tumorigenesis of the colon.

Acknowledgments

We thank Kyoko Takahashi, Ayako Suga, and Yoshitaka Kinjo for their technical assistance. This study was supported by grants from the Ministry of Education, Culture, Sports, Science and Technology of Japan, and grants from PRESTO, and from the Ministry of Health, Labour and Welfare of Japan.

Disclosure Statement

The authors have no conflict of interest to declare.

References

1 Chong JA, Tapia-Ramirez J, Kim S *et al.* REST: a mammalian silencer protein that restricts sodium channel gene expression to neurons. *Cell* 1995; **80**: 949–57.
2 Schoenherr CJ, Anderson DJ. The neuron-restrictive silencer factor (NRSF): a coordinate repressor of multiple neuron-specific genes. *Science* 1995; **267**: 1360–3.
3 Ballas N, Grunseich C, Lu DD, Speh JC, Mandel G. REST and its corepressors mediate plasticity of neuronal gene chromatin throughout neurogenesis. *Cell* 2005; **121**: 645–57.
4 Jones FS, Meech R. Knockout of REST/NRSF shows that the protein is a potent repressor of neuronally expressed genes in non-neural tissues. *Bioessays* 1999; **21**: 372–6.
5 Coulson JM. Transcriptional regulation: cancer, neurons and the REST. *Curr Biol* 2005; **15**: 665–8.
6 Majumder S. REST in good times and bad: roles in tumor suppressor and oncogenic activities. *Cell Cycle* 2006; **5**: 1929–35.
7 Weissman AM. How much REST is enough? *Cancer Cell* 2008; **13**: 381–3.
8 Tawadros T, Martin D, Abderrahmani A, Leisinger HJ, Waeber G, Haefliger JA. IB1/JIP-1 controls JNK activation and increased during prostatic LNCaP cells neuroendocrine differentiation. *Cell Signal* 2005; **17**: 929–39.
9 Reddy BY, Greco SJ, Patel PS, Trzaska KA, Rameshwar P. RE-1-silencing transcription factor shows tumor-suppressor functions and negatively regulates the oncogenic TAC1 in breast cancer cells. *Proc Natl Acad Sci USA* 2009; **106**: 4408–13.
10 Wagoner MP, Gunsalus KT, Schoenike B, Richardson AL, Friedl A, Roopra A. The transcription factor REST is lost in aggressive breast cancer. *PLoS Genet* 2010; **6**: e1000979.
11 Lv H, Pan G, Zheng G *et al.* Expression and functions of the repressor element 1 (RE-1)-silencing transcription factor (REST) in breast cancer. *J Cell Biochem* 2010; **110**: 968–74.
12 Coulson JM, Edgson JL, Woll PJ, Quinn JP. A splice variant of the neuron-restrictive silencer factor repressor is expressed in small cell lung cancer: a potential role in derepression of neuroendocrine genes and a useful clinical marker. *Cancer Res* 2000; **60**: 1840–4.
13 Gurrola-Diaz C, Lacroix J, Dihlmann S, Becker CM, von Knebel Doeberitz M. Reduced expression of the neuron restrictive silencer factor permits transcription of glycine receptor alpha1 subunit in small-cell lung cancer cells. *Oncogene* 2003; **22**: 5636–45.
14 Neumann SB, Seitz R, Gorzella A, Heister A, Doeberitz MK, Becker CM. Relaxation of glycine receptor and onconeural gene transcription control in NRSF deficient small cell lung cancer cell lines. *Brain Res Mol Brain Res* 2004; **120**: 173–81.
15 Moss AC, Jacobson GM, Walker LE, Blake NW, Marshall E, Coulson JM. SCG3 transcript in peripheral blood is a prognostic biomarker for REST-deficient small cell lung cancer. *Clin Cancer Res* 2009; **15**: 274–83.
16 Kreisler A, Strissel PL, Strick R, Neumann SB, Schumacher U, Becker CM. Regulation of the NRSF/REST gene by methylation and CREB affects the cellular phenotype of small-cell lung cancer. *Oncogene* 2010; **29**: 5828–38.
17 Lawinger P, Venugopal R, Guo ZS *et al.* The neuronal repressor REST/NRSF is an essential regulator in medulloblastoma cells. *Nat Med* 2000; **6**: 826–31.
18 Fuller GN, Su X, Price RE *et al.* Many human medulloblastoma tumors overexpress repressor element-1 silencing transcription (REST)/neuron-restrictive silencer factor, which can be functionally countered by REST-VP16. *Mol Cancer Ther* 2005; **4**: 343–9.

19 Su X, Gopalakrishnan V, Stearns D *et al.* Abnormal expression of REST/NRSF and Myc in neural stem/progenitor cells causes cerebellar tumors by blocking neuronal differentiation. *Mol Cell Biol* 2006; **26**: 1666–78.
20 Nishimura E, Sasaki K, Maruyama K, Tsukada T, Yamaguchi K. Decrease in neuron-restrictive silencer factor (NRSF) mRNA levels during differentiation of cultured neuroblastoma cells. *Neurosci Lett* 1996; **211**: 101–4.
21 Palm K, Metsis M, Timmusk T. Neuron-specific splicing of zinc finger transcription factor REST/NRSF/XBR is frequent in neuroblastomas and conserved in human, mouse and rat. *Brain Res Mol Brain Res* 1999; **72**: 30–9.
22 Donev RM, Gray LC, Sivasankar B, Hughes TR, Van den Berg CW, Morgan BP. Modulation of CD59 expression by restrictive silencer factor-derived peptides in cancer immunotherapy for neuroblastoma. *Cancer Res* 2008; **68**: 5979–87.
23 Lietz M, Cicchetti P, Thiel G. Inverse expression pattern of REST and synapsin I in human neuroblastoma cells. *Biol Chem* 1998; **379**: 1301–4.
24 Westbrook TF, Martin ES, Schlabach MR *et al.* A genetic screen for candidate tumor suppressors identifies REST. *Cell* 2005; **121**: 837–48.
25 Chen ZF, Paquette AJ, Anderson DJ. NRSF/REST is required *in vivo* for repression of multiple neuronal target genes during embryogenesis. *Nat Genet* 1998; **20**: 136–42.
26 Yamada Y, Aoki H, Kunisada T, Hara A. Rest promotes the early differentiation of mouse ESCs but is not required for their maintenance. *Cell Stem Cell* 2010; **6**: 10–5.
27 Andres ME, Burger C, Peral-Rubio MJ *et al.* CoREST: a functional corepressor required for regulation of neural-specific gene expression. *Proc Natl Acad Sci USA* 1999; **96**: 9873–8.
28 Lin H, Yamada Y, Nguyen S *et al.* Suppression of intestinal neoplasia by deletion of Dnmt3b. *Mol Cell Biol* 2006; **26**: 2976–83.
29 Sakai H, Yamada Y, Shimizu M, Saito K, Moriwaki H, Hara A. Genetic ablation of Tnfalpha demonstrates no detectable suppressive effect on inflammation-related mouse colon tumorigenesis. *Chem Biol Interact* 2010; **184**: 423–30.
30 Yamada Y, Mori H. Multistep carcinogenesis of the colon in Apc(Min/+) mouse. *Cancer Sci* 2007; **98**: 6–10.
31 Yamada Y, Jackson-Grusby L, Linhart H *et al.* Opposing effects of DNA hypomethylation on intestinal and liver carcinogenesis. *Proc Natl Acad Sci USA* 2005; **102**: 13580–5.
32 Laird PW, Jackson-Grusby L, Fazeli A *et al.* Suppression of intestinal neoplasia by DNA hypomethylation. *Cell* 1995; **81**: 197–205.
33 Linhart HG, Lin H, Yamada Y *et al.* Dnmt3b promotes tumorigenesis *in vivo* by gene-specific de novo methylation and transcriptional silencing. *Genes Dev* 2007; **21**: 3110–22.
34 Huang Y, Myers SJ, Dingledine R. Transcriptional repression by REST: recruitment of Sin3A and histone deacetylase to neuronal genes. *Nat Neurosci* 1999; **2**: 867–72.
35 Naruse Y, Aoki T, Kojima T, Mori N. Neural restrictive silencer factor recruits mSin3 and histone deacetylase complex to repress neuron-specific target genes. *Proc Natl Acad Sci USA* 1999; **96**: 13691–6.
36 Roopra A, Sharling L, Wood IC *et al.* Transcriptional repression by neuron-restrictive silencer factor is mediated via the Sin3-histone deacetylase complex. *Mol Cell Biol* 2000; **20**: 2147–57.
37 Shi Y, Sawada J, Sui G *et al.* Coordinated histone modifications mediated by a CtBP co-repressor complex. *Nature* 2003; **422**: 735–8.
38 Shi Y, Lan F, Matson C *et al.* Histone demethylation mediated by the nuclear amine oxidase homolog LSD1. *Cell* 2004; **119**: 941–53.
39 Lunyak VV, Burgess R, Prefontaine GG *et al.* Corepressor-dependent silencing of chromosomal regions encoding neuronal genes. *Science* 2002; **298**: 1747–52.
40 Bruce AW, Donaldson IJ, Wood IC *et al.* Genome-wide analysis of repressor element 1 silencing transcription factor/neuron-restrictive silencing factor (REST/NRSF) target genes. *Proc Natl Acad Sci USA* 2004; **101**: 10458–63.
41 Bernick PE, Klimstra DS, Shia J *et al.* Neuroendocrine carcinomas of the colon and rectum. *Dis Colon Rectum* 2004; **47**: 163–9.

doi: 10.1111/j.1349-7006.2011.02006.x

Published OnlineFirst September 27, 2011; DOI:10.1158/1940-6207.CAPR-11-0096

Research Article

Cancer Prevention Research

Revisit of Field Cancerization in Squamous Cell Carcinoma of Upper Aerodigestive Tract: Better Risk Assessment with Epigenetic Markers

Yi-Chia Lee[1,5], Hsiu-Po Wang[1], Cheng-Ping Wang[2], Jenq-Yuh Ko[2], Jang-Ming Lee[3], Han-Mo Chiu[1], Jaw-Town Lin[1,6], Satoshi Yamashita[7], Daiji Oka[7,8], Naoko Watanabe[7], Yasunori Matsuda[7], Toshikazu Ushijima[7], and Ming-Shiang Wu[1,4]

Abstract

We quantified field cancerization of squamous cell carcinoma in the upper aerodigestive tract with epigenetic markers and evaluated their performance for risk assessment. Methylation levels were analyzed by quantitative methylation-specific PCR of biopsied specimens from a training set of 255 patients and a validation set of 224 patients. We also measured traditional risk factors based on demographics, lifestyle, serology, genetic polymorphisms, and endoscopy. The methylation levels of four markers increased stepwise, with the lowest levels in normal esophageal mucosae from healthy subjects without carcinogen exposure, then normal mucosae from healthy subjects with carcinogen exposure, then normal mucosae from cancer patients, and the highest levels were in cancerous mucosae ($P < 0.05$). Cumulative exposure to alcohol increased methylation of homeobox A9 in normal mucosae ($P < 0.01$). Drinkers had higher methylation of ubiquitin carboxyl-terminal esterase L1 and metallothionein 1M ($P < 0.05$), and users of betel quid had higher methylation of homeobox A9 ($P = 0.01$). Smokers had increased methylation of all four markers ($P < 0.05$). Traditional risk factors allowed us to discriminate between patients with and without cancers with 74% sensitivity (95% CI: 67%–81%), 74% specificity (66%–82%), and 80% area under the curve (67%–91%); epigenetic markers in normal esophageal mucosa had values of 74% (69%–79%), 75% (67%–83%), and 83% (79%–87%); and both together had values of 82% (76%–88%), 81% (74%–88%), and 91% (88%–94%). Epigenetic markers done well in the validation set with 80% area under the curve (73%–85%). We concluded that epigenetics could improve the accuracies of risk assessment. *Cancer Prev Res; 4(12); 1982–92. ©2011 AACR.*

Introduction

Squamous cell carcinoma (SCC) is the major phenotype of esophageal cancer in Asia. Survival of this cancer is decreased because of field cancerization, in which synchronous and metachronous cancers occur in the upper aerodigestive tract (UADT; ref. 1). Screening and surveillance measures, particularly the use of sophisticated endoscopic technologies such as narrow-band imaging and Lugol staining (2), currently aid physicians in starting early intervention and providing curative treatment.

The populations of patients exposed to well-established risk factors may outnumber the capacity of endoscopists to screen them. For instance, among the adult male population in Taiwan, 46% drink alcohol, 15% chew betel quid, and 57% smoke cigarettes (3), which are all behaviors that result in an increased incidence of SCC (4). Following a negative endoscopy, an efficient risk-assessment method is needed to design surveillance programs for early detection of superficial SCC in the head and neck region and esophagus (2). However, past efforts based on demographic characteristics (5–7), lifestyle risk factors (8, 9), genetic susceptibilities (10–14), serological markers (15–18), and endoscopic findings (19), alone or in combination (15, 20, 21), have not produced models efficient enough to be effective.

Aberrant DNA methylation in histologically normal mucosae has attracted attention as an indicator of past

Authors' Affiliations: Departments of [1]Internal Medicine, [2]Otolaryngology, [3]Surgery, and [4]Primary Care Medicine, College of Medicine; [5]Division of Biostatistics, College of Public Health, National Taiwan University, Taipei, Taiwan; [6]Department of Internal Medicine, E-DA Hospital and I-Shou University, Kaohsiung County, Taiwan; [7]Division of Epigenomics, National Cancer Center Research Institute; and [8]Department of Gastrointestinal Surgery, Graduate School of Medicine, University of Tokyo, Tokyo, Japan

Note: Supplementary data for this article are available at Cancer Prevention Research Online (http://cancerprevres.aacrjournals.org/).

Presented in Part: Digestive Disease Week Conference, Chicago, USA, 7–10 May 2011 (abstract: Su1129).

Corresponding Authors: Ming-Shiang Wu, Department of Internal Medicine, National Taiwan University Hospital, 7, Chung-Shan South Road, Taipei, Taiwan. Phone: 886-2-23123456 (ext.) 65695; Fax: 886-2-23947899; E-mail: mingshiang@ntu.edu.tw and Toshikazu Ushijima, Division of Epigenomics, National Cancer Center Research Institute, 5-1-1 Tsukiji, Chou-Ku, Tokyo 104-0045, Japan; E-mail: tushijim@ncc.go.jp

doi: 10.1158/1940-6207.CAPR-11-0096

Published OnlineFirst September 27, 2011; DOI:10.1158/1940-6207.CAPR-11-0096

exposure to carcinogens and as a marker for future risk prediction (22). Reliable measuring techniques, such as real-time quantitative methylation-specific PCR (qMSP), have been confirmed to be sensitive and accurate in quantifying this early carcinogenic event (23). They offer an opportunity to elucidate whether aberrant DNA methylation can serve as a marker to quantify the field effects associated with SCC of the UADT. If this hypothesis is found to be true, we can compare the performance of risk-assessment methods based on epigenetic markers with those based on traditional risk factors. We also validated the performance of the epigenetic markers with a prospectively recruited independent cohort.

Materials and Methods

Subjects and study design

We recruited consecutive Taiwanese patients who received endoscopic screening at the National Taiwan University Hospital between January 2008 and May 2011 due to UADT symptoms, such as globus sensation and dysphagia. This cohort was split into a training set to develop a risk-assessment model for UADT cancer based on epigenetic markers and a validation set to evaluate model performance. Our initial pilot experiment determined the required sample size for hypothesis testing with 123 biopsied samples from 103 patients. The study protocol included thoroughly evaluating traditional risk factors, screening by endoscopy, and quantifying DNA methylation in the biopsied specimens. All participants provided informed consent, and the Ethics Committee of the National Taiwan University Hospital approved the study (no: 200706034R and 200806039R).

Traditional risk factors

Prior to the endoscopic screening, patients underwent face-to-face interviews, physical examinations, and laboratory tests to identify traditional risk factors for SCCs in the head and neck region (24) and in the esophagus (25) that would be used as baseline comparators for the upcoming epigenetic approach. These included: the demographic characteristics (6, 7) of age, sex, and body mass index (BMI); the lifestyle risk factors (8, 9, 11) of alcohol drinking, betel quid chewing, and cigarette smoking (briefly as "ABC"); polymorphisms in genes encoding enzymes involved in the metabolism of alcohol (10–13), including aldehyde dehydrogenase (*ALDH*) 2, alcohol dehydrogenase (*ADH*) *1B*, and *ADH 1C*; polymorphisms in genes encoding enzymes involved in the metabolism of xenobiotics (14), including glutathione S transferase (*GST*) *P1*, *GST M1*, and *GST T1*; and serological markers (15–18), including increased mean corpuscular volume (MCV), *Helicobacter pylori* infection, and human papillomavirus infection.

Lifestyle risk factors were recorded according to frequency (alcohol where one time indicates at least 15.75 gm of ethanol: 0, never; 1, once per week; 2, once to twice per week; 3, 3–4 times per week; and 4, 5 or more times per week; betel quid: 0, never; 1, less than 1 piece daily; 2, 1–10 pieces daily; 3, 11 to 20 pieces daily; and 4, more than 20 pieces daily; cigarettes: 0, never; 1, less than 0.5 pack daily; 2, 0.5–1 pack daily; 3, 1–2 packs daily; and 4, more than 2 packs daily) and duration (0, never; 1, less than 1 year; 2, 1–10 years; 3, 11–20 years; and 4, more than 20 years). The cumulative lifetime exposure was calculated by multiplying the frequency and duration, and then categorized into 3 levels: level 1, never (0); level 2, light to moderate (1–11); and level 3, heavy ($\geq$12). Polymorphic genotypes were determined from peripheral blood leucocytes with PCR-RFLP (the primers are provided in the Supplementary Table S1). Diagnosis of *H. pylori* infection was made histologically or serologically (Diagnostic Products Co.; ref. 26) as appropriate. Human papillomavirus infection was serologically diagnosed by ELISA with commercially available kits (Wuhan EIAab Science Co., Ltd.; ref. 27). The cutoff value for human papillomavirus IgG was set at 600 U/mL based on 3 SDs above the mean optical density obtained from serum samples of negative controls.

Endoscopic examination and tissue sampling

After evaluating traditional risk factors, patients underwent endoscopic examinations by white-light, narrow-band imaging, and Lugol staining in a single session, which is a method shown to be accurate in the detection of cancers of the UADT (28, 29). We evaluated endoscopic findings of numerous irregular-shaped multiform unstained areas over the background esophageal mucosae, namely, Lugol voiding lesions (LVL) after spraying of Lugol solution (19), as one of the traditional risk factors. A biopsy was done on any suspicious lesions along the UADT before chemotherapy or radiation therapy and also on normal-appearing mucosae in the esophagus. Normal-appearing mucosa was defined as an area that did not seem brownish ("brownish" indicated microvascular proliferation) under narrow-band imaging and, after being sprayed with Lugol's solution, was stained ("unstained" indicated glycogen depletion). For patients with either head and neck cancer or esophageal cancer, biopsies for normal-appearing mucosae were routinely done 3 cm above the squamocolumnar junction in the esophagus; in cases with neoplastic lesions close to this area, the biopsy sites were moved to at least 5 cm away from the neoplastic margin. In addition to histologic confirmation, a set of specimens was stored at −80°C until genomic DNA was extracted.

Internally validating epigenetic markers and quantifying DNA methylation levels

Genomic DNA was sent to the National Cancer Center Research Institute in Japan. The DNA methylation of the epigenetic markers was quantified with the qMSP. The laboratory work was similar to the details previously reported that used an independent test set of 60 tumor samples derived from Japanese individuals (30). In brief, 14 genes whose promoter CpG islands were methylated in esophageal SCCs were isolated by a genome-wide screening of genes reexpressed after esophageal SCC cell lines were treated with the demethylating agent 5-aza-2′-deoxycytidine. Most of the

Published OnlineFirst September 27, 2011; DOI:10.1158/1940-6207.CAPR-11-0096

14 genes were also methylated at low levels in adjacent esophageal mucosae. We analyzed 4 genes correlated with smoking duration in this study: homeobox A9 (*HOXA9*), neurofilament heavy polypeptide (*NEFH*, 200 kDa), ubiquitin carboxyl-terminal esterase L1 (*UCHL1*), and metallothionein 1M (*MT1M*).

Laboratory analyses were done by laboratory technicians who were blinded to the clinical status of the samples analyzed. As in our previous report (30), DNA was digested by *Bam*HI, denatured, and treated by 15 cycles denaturing for 30 seconds at 95°C and incubating for 15 minutes at 50°C in 3.1 N sodium bisulfite (pH 5.0) and 0.5 mmol/L hydroquinone. The samples were desalted and then desulfonated in 0.3 N NaOH. The qMSP was done with primer sets specific to either the methylated or unmethylated sequence (M or U set) with the sodium bisulfite-treated DNA and an iCycler Thermal Cycler (Bio-Rad Laboratories). We compared the amplification of sample DNA to that of standard DNA that was prepared from a plasmid with a cloned PCR product and that had known copy numbers of the cloned DNA. The amount of methylated and unmethylated DNA in the sample was quantified.

Statistical analysis

Data are expressed as average ± SD (median; range) for continuous variables and as a percentage for categorical variables. The measurement of DNA methylation levels in the biopsied specimens was the starting point for the following statistical analyses: (i) comparing methylation levels according to stage of carcinogenic sequence and level of carcinogen exposure; (ii) building logistic-regression models to determine the likelihood of UADT cancers based on epigenetic markers, traditional risk factors, and both together; and (iii) comparing the predictive value of epigenetic markers on a validation set of patients not used in the initial model building phase.

First, the ability of each epigenetic marker to serve as an indicator for the field effects was confirmed by seeking a stepwise relationship among the methylation levels that followed the carcinogenic sequence related to the chronic irritation of ABC, which are the 3 principal determinants of SCC. We simulated the carcinogenic sequence by categorizing the biopsied specimens into 4 groups: group 1, normal esophageal mucosae of healthy subjects with no exposure to ABC; group 2, normal esophageal mucosae of healthy subjects with at least one of the above exposures; group 3, normal esophageal mucosae of cancer patients; and group 4, cancerous mucosae. Methylation levels were expected to increase in a stepwise manner in linear regression analyses as the group number increased. Scatter plots were drawn to describe the results. Pairwise comparisons between groups were also made using the nonparametric Mann–Whitney *U* test. We also correlated methylation levels in the normal-appearing esophageal mucosae (i.e., groups 1, 2, and 3) with cumulative lifetime exposures to ABC. Tests for linear trends and pairwise comparisons between subjects with different exposure levels were done in a similar manner. In cancerous tissues (i.e., group 4), the association between methylation levels and clinicopathologic characteristics was evaluated.

Second, the predictive value of our epigenetic markers was assessed by developing logistic-regression models that used the methylation levels in normal-appearing esophageal mucosae to predict the probability of a patient having head and neck cancer, esophageal cancer, and UADT cancer based on the training samples. Following univariate logistic-regression analyses, an epigenetic model was built using backward elimination of predictors from the full 4-predictor model that excluded those with $P \geq 0.05$. We excluded strong linear dependencies among the predictors by examining tolerance and the variance inflation factor. We also excluded the statistical significance of interactions and nonlinear terms.

We developed logistic-regression models using the traditional risk factors to compare with the epigenetic model. Continuous predictors included age, BMI, levels of cumulative lifetime exposures to ABC, and MCV. For the categorical predictors, the baseline comparators were: female, unexposed to ABC, without *H. pylori* infection, without human papillomavirus infection, and carrying these genotypes: *ALDH2*1/2*1* (fast metabolizers), *ADH1B*1/*2* or **2/*2* (fast), *ADH1C*1/*2* or **2/*2* (slow), *GSTP1 ile/val* or *val/val* (fast), *GSTM1 present* (active), and *GSTT1 present* (active). Univariate logistic-regression analyzed each predictor and those predictors with $P < 0.05$ were included in a multivariate regression model. We also assessed interaction terms, in particular, between the polymorphic genotypes and exposures to ABC. A traditional model for the probability of a patient having UADT cancer was built using backward elimination based on Akaike's information criterion.

To further assess if our epigenetic markers improved on or added value to the traditional methods, we added the epigenetic markers individually to the final traditional model and determined the independence and magnitude of the contribution of the epigenetic markers after adjusting for the effects of traditional risk factors. A combined model was constructed based on Akaike's information criterion. The significance of each predictor is presented as an OR and a 95% CI. A 2-tailed $P < 0.05$ indicated statistical significance. All statistical analyses were done using the SAS software system, version 9.2 (SAS Institute Inc.).

The performance of the above predictive models was compared by graphically displaying their relative performances on a receiver operating characteristic (ROC) curve that plotted the sensitivity against the false-positive rate (i.e., 1-specificity) over a range of cutoff values. The area under the curve (AUC) measured the performance of the test in correctly distinguishing subjects with and without cancer and the corresponding 95% CIs were calculated using 1,000 bootstrap sample sets (drawn with replacement) of the same size of the original dataset (31). The model calibration was assessed using the Hosmer–Lemeshow test for goodness of fit, which evaluated whether the predicted probabilities agreed with the observed probabilities in deciles. The bootstrap method evaluated statistical differences between the

Published OnlineFirst September 27, 2011; DOI:10.1158/1940-6207.CAPR-11-0096

AUCs of epigenetic, traditional, and combined models over the same training set. We determined the optimal cutoff value for each model by selecting the point closest to theoretically perfect performance in discrimination and calculated the corresponding sensitivity and specificity pair.

Finally, to validate the epigenetic model, we recruited an independent validation set of a sample size similar to the training set at the National Taiwan University Hospital and quantified their DNA methylation levels in normal esophageal mucosae in a similar manner. We fitted an epigenetic model using the training set, saved the details of the fitted model such as the parameter estimates and SEs, and tested its performance on the validation set. The derived AUC was compared with that based on the training set using the z test.

Sample size estimation

The sample size of this prospective study was planned previously based on our previous study (30). That study found that methylation levels in the normal esophageal mucosae of cancer patients (i.e., group 3) were 2.7% ± 2.5% (average ± SD; median: 2.4%; range: 0%–16.3%) for *HOXA9*, 7.2% ± 5.1% (6.2%; 0.4%–20.3%) for *NEFH*, 1.8% ± 3.6% (0.9%; 0%–22.4%) for *UCHL1*, and 1.9% ± 1.7% (1.3%; 0%–6.8%) for *MT1M*. However, the methylation levels of healthy controls (i.e., groups 1 and 2) were not available. To test the hypothesis that methylation levels in the normal esophageal mucosae could differentiate cancer patients from noncancer subjects, we used the initial 10 healthy controls in the pilot experiment to estimate the required sample size; their average methylation levels were 1.2% for *HOXA9*, 0.2% for *NEFH*, 0.2% for *UCHL1*, and 0.6% for *MT1M*. To detect a significant difference between the case (i.e., group 3) and control (i.e., groups 1 and 2) at $\alpha = 0.05$, $\beta = 0.2$, and a single-tail hypothesis, it was estimated that a total of 64 samples for each group would suffice using the Student t test. To compare the model based on epigenetic markers with the one based on traditional risk factors, we set a minimally acceptable level of accuracy at 80%: that is, a level that is commonly considered a prerequisite for population-based screening. Knowing that the average accuracy of traditional methods was approximately 70% (5, 20), an overall sample size of 231 was required to detect this difference at $\alpha = 0.05$ and $\beta = 0.2$ using the χ^2 test. The sample size estimation was done using the nQuery Advisor 7.0.

Results

Patients' characteristics

Between January 2008 and April 2009, 272 consecutive patients were screened. Seventeen (6.3%) subjects were excluded, including 8 having a history of bleeding tendency, 2 with failed endoscopic examination, and 7 refusing endoscopic biopsy. The remaining 255 patients were recruited to the study as the training set. The demographic and clinicopathologic characteristics between cases and controls are shown in the Table 1. Histories of ABC were confirmed in 190 (74.5%) subjects; among them, 66 (34.7%) were double positives and 84 (42.2%) were triple positives. Of the 146 (57.3%) patients diagnosed with SCC of the UADT, 49 were diagnosed with head and neck cancer (including 4 with oral cavity cancer, 2 with laryngeal cancer, and 43 with hypopharyngeal cancer), 91 with esophageal cancer, and 6 patients with synchronous head and neck and esophageal cancers. Of the 109 subjects who had undergone the similar diagnostic procedures but had negative results, 46 (42.2%) had no history of ABC while 63 (57.8%) had used at least one of these 3 risk factors.

Quantifying field effects with epigenetic markers

A total of 397 biopsied specimens were obtained in the training cohort and DNA methylation levels were successfully quantified in 372 (93.7%) of them. The methylation levels of all 4 epigenetic markers increased in a stepwise manner ($P < 0.001$) based on the exposure to alcohol, betel quid, or cigarettes (Fig. 1). The normal esophageal mucosae of healthy subjects not exposed to alcohol, betel quid, or cigarette (group 1) had methylation levels of 2.8% ± 3.2% (average ± SD; median: 1.8%; range: 0.3%–15.4%) for *HOXA9*, 0.4% ± 0.7% (0.2%; 0%–4.1%) for *NEFH*, 0.3% ± 0.5% (0.2%; 0%–2.4%) for *UCHL1*, and 0.9% ± 1.7% (0.4%; 0.1%–10.7%) for *MT1M*. The normal esophageal mucosae of healthy subjects with at least one of the above exposures (group 2) had methylation levels of 4.8% ± 5.7% (2.7%; 0.2%–29.3%) for *HOXA9*, 0.6% ± 1.1% (0.3%; 0%–7.4%) for *NEFH*, 1.2% ± 3.3% (0.3%; 0%–23.7%) for *UCHL1*, and 1.0% ± 0.7% (0.9%; 0%–3.1%) for *MT1M*. The normal esophageal mucosae of cancer patients (group 3) had methylation levels of 9.2% ± 9.9% (5.8%; 0%–65.8%) for *HOXA9*, 0.7% ± 1.0% (0.4%; 0%–7.3%) for *NEFH*, 2.0% ± 5.0% (0.4%; 0%–42.8%) for *UCHL1*, and 1.4% ± 2.2% (0.9%; 0.1%–18.0%) for *MT1M*.

Methylation levels in the normal esophageal mucosae correlated to cumulative lifetime exposures to ABC (Supplementary Figs. S1–7). Notably, a dose-dependent relationship was noted between the methylation levels of *HOXA9* and alcohol consumption ($P < 0.01$). The methylation levels of *UCHL1* and *MT1M* were higher in drinkers ($P < 0.05$). Although we did not identify a linear relationship between the methylation levels and dosage of betel quid use or cigarette smoking, betel quid users had significantly higher *HOXA9* methylation levels than nonusers ($P = 0.01$) and smokers had consistently higher methylation levels for the 4 markers ($P < 0.05$). Regarding the concurrent use of ABC, the methylation levels of 4 marker genes were higher in individuals who had at least one risk factor ($P \leq 0.01$). The methylation levels of *HOXA9* increased in a stepwise manner with the number of exposures ($P < 0.01$), suggesting an additive effect.

When the data was stratified by the presence of numerous LVLs, which are a well-recognized indicator of SCC risk, higher methylation levels were noted in the cases with numerous LVLs (Supplementary Fig. S8), and the levels of the *HOXA9* and *UCHL1* genes reached statistical significance ($P < 0.01$). Stratifying the data by infection with *H. pylori* or human papillomavirus did not yield significant differences in the methylation levels of noncancerous mucosae.

Published OnlineFirst September 27, 2011; DOI:10.1158/1940-6207.CAPR-11-0096

Table 1. Patient characteristics of the training set

Parameters	Controls ($n = 109$)	Cases ($n = 146$)	Total ($n = 255$)
Demographic characteristics			
Age, mean ± SD, range (y)	59.8 ± 14.3, 25–90	59.8 ± 10.7, 32–89	59.5 ± 12.4, 25–90
Male sex (%)	78 (71.6)	136 (93.2)	214 (83.9)
BMI, mean ± SD, range (kg/m^2)	23.0 ± 3.5, 17.0–33.1	22.1 ± 3.4, 15.6–34.3	22.5 ± 3.5, 15.6–34.3
Lifestyle risk factors (%)	57 (52.3)	133 (91.1)	190 (74.5)
Levels of alcohol drinking			
Never	70 (64.2)	24 (16.4)	94 (36.9)
Light to moderate	26 (23.9)	36 (24.7)	62 (24.3)
Heavy	13 (11.9)	86 (58.9)	99 (38.8)
Levels of betel quid chewing			
Never	92 (84.4)	65 (44.5)	157 (61.6)
Light to moderate	7 (6.4)	30 (20.6)	37 (14.5)
Heavy	10 (9.2)	51 (34.9)	61 (23.9)
Levels of cigarette smoking			
Never	68 (62.4)	24 (16.5)	92 (36.1)
Light to moderate	20 (18.3)	56 (38.3)	76 (29.8)
Heavy	21 (19.3)	66 (45.2)	87 (34.1)
Genetic polymorphisms (%)			
Encoding enzymes in the metabolism of alcohol			
ALDH2 genotype	41 (37.6)	128 (87.7)	169 (66.3)
*ALDH2*1/2*1*, fast	15 (36.6)	36 (28.1)	51 (30.2)
*ALDH2*1/2*2* or *2*2/2*2*, slow	26 (63.4)	92 (71.9)	118 (69.8)
ADH1B genotype	39 (35.8)	128 (87.7)	167 (65.5)
*ADH1B*1/*1*, slow	4 (10.3)	37 (28.9)	41 (24.6)
*ADH1B*1/*2* or **2/*2*, fast	35 (89.7)	91 (71.1)	126 (75.4)
ADH1C genotype	38 (34.9)	126 (86.3)	164 (57.3)
*ADH1C*1/*1*, fast	34 (89.5)	101 (80.2)	135 (82.3)
*ADH1C*1/*2* or **2/*2*, slow	4 (10.5)	25 (19.8)	29 (17.7)
Encoding enzymes in the metabolism of xenobiotics			
GSTP1 genotype	36 (33.0)	121 (82.9)	157 (61.6)
ile/ile, slow	31 (86.1)	90 (74.4)	121 (77.1)
ile/val or *val/val*, fast	5 (13.9)	31 (25.6)	36 (22.9)
GSTM1 genotype	40 (36.7)	128 (87.7)	168 (65.9)
present, active	19 (47.5)	54 (42.2)	73 (43.5)
null, inactive	21 (52.5)	74 (57.8)	95 (56.5)
GSTT1 genotype	41 (37.6)	128 (87.7)	169 (66.3)
present, active	20 (48.8)	62 (48.4)	82 (48.5)
null, inactive	21 (51.2)	66 (51.6)	87 (51.5)
Serological markers			
MCV, mean ± SD, range (fL)	89.3 ± 8.3, 63.5–104.1	93.0 ± 6.9, 67.1–111.5	92.0 ± 7.7, 63.5–111.5
H. pylori infections (%)	40/103 (38.8)	70/141 (49.7)	110/244 (45.1)
Human papillomavirus infections (%)	7/41 (17.1)	30/128 (23.4)	37/169 (21.9)
Endoscopic findings (%)			
Negative study	109	0	109 (42.7)
Head and neck SCC	0	49 (33.6)	49 (19.2)
Esophageal SCC	0	91 (62.3)	91 (35.7)
Synchronous head and neck and esophageal SCC	0	6 (4.1)	6 (2.4)
Presence of numerous LVLs in the background mucosae	6 (10.5)	68 (48.6)	74 (29.0)

The cancerous mucosae (group 4) had methylation levels of 33.2% ± 24.7% (28.8%; 0%–87.6%) for *HOXA9*, 6.4% ± 10.0% (2.3%; 0%–54.9%) for *NEFH*, 18.1% ± 23.7% (3.9%; 0%–91.4%) for *UCHL1*, and 11.5% ± 16.7% (2.0%; 0.1%–73.9%) for *MT1M*, which was a broad distribution with higher average values than each of the 3 normal groups

Published OnlineFirst September 27, 2011; DOI:10.1158/1940-6207.CAPR-11-0096

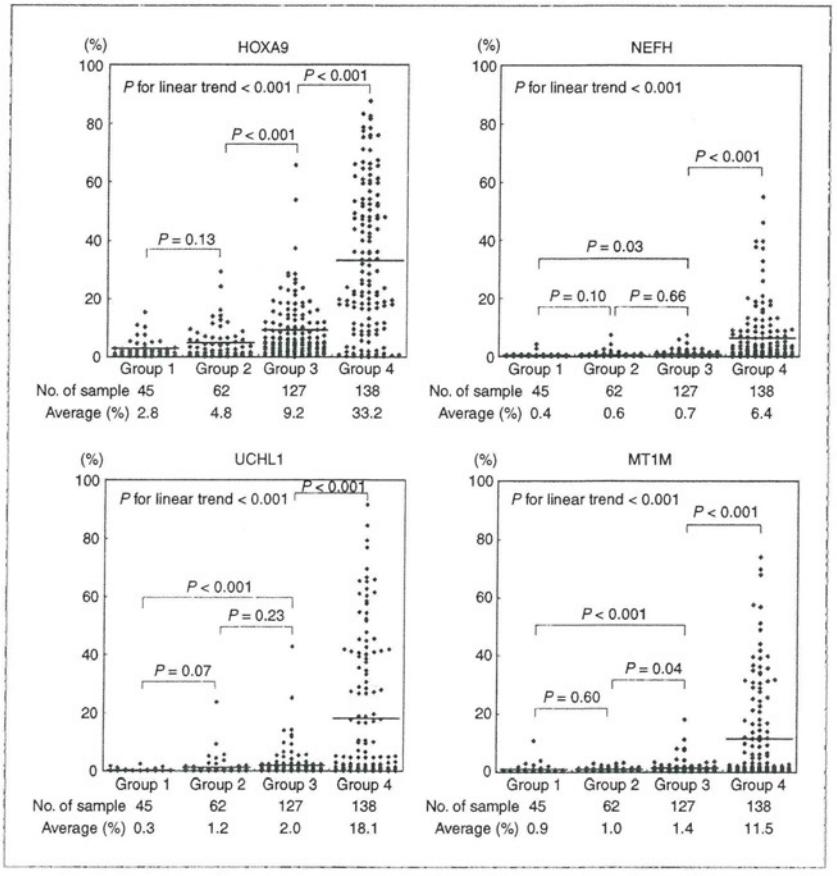

Figure 1. Methylation levels of the epigenetic markers along the carcinogenic sequence in the training set. Group 1, normal esophageal mucosae of healthy subjects without exposure to alcohol, betel quid, or cigarette; group 2, normal esophageal mucosae of healthy subjects with at least one of the above exposures; group 3, normal esophageal mucosae of cancer patients; group 4, cancerous mucosae.

($P < 0.001$). Cancers of the head and neck and of the esophagus had similar methylation levels (Supplementary Fig. S9). No association was found between methylation levels and clinicopathologic characteristics, including TNM staging, tumor differentiation, and multiplicity (data not shown).

Comparing performance between head and neck cancer and esophageal cancer

Methylation levels in the normal esophageal mucosae were significantly associated with the risk of SCC for the 4 epigenetic markers (Table 2). To predict head and neck cancer, AUCs for each of the epigenetic markers were 83% for *HOXA9* (bootstrap 95% CI: 77%–88%), 69% for *NEFH* (60%–74%), 67% for *UCHL1* (59%–74%), and 74% for *MT1M* (67%–81%). To predict esophageal cancer, similarly, the AUCs were 78% for *HOXA9* (73%–83%), 71% for *NEFH* (65%–77%), 73% for *UCHL1* (67%–78%), and 71% for *MT1M* (65%–77%). Overall, to predict UADT cancer, the AUCs for each of the markers were 80% for *HOXA9* (75%–84%), 69% for *NEFH* (64%–75%), 71% for *UCHL1* (66%–76%), and 72% for *MT1M* (66%–77%). Notably, *HOXA9* showed the best discriminative ability and an additional dichotomous analysis showed that OR was 10.189 (5.430–19.118) when the cutoff point of the *HOXA9* methylation level was set at 9.2% (the average value of cancer group).

An optimal epigenetic model to predict UADT cancer was constructed with 2 predictors of *HOXA9* and *NEFH* methylation levels (AUC: 83%; bootstrap 95% CI: 79%–86%). The model had similar performances for head and neck cancer and for esophageal cancer (Supplementary Fig. S10). The sensitivity, specificity, and AUC were 76% (65%–87%), 75% (67%–83%), and 85% (80%–90%), respectively, in predicting head and neck cancer, and 72% (63%–81%), 73% (65%–81%), and 82% (77%–87%), respectively, in predicting esophageal cancer.

Thus, we confirmed that our 4 epigenetic markers were robust as a quantitative measure for field cancerization along the UADT.

Comparing performance between traditional risk factors and epigenetic markers

The traditional risk factors were compared between cases and controls using univariate logistic-regression analyses (Table 2). Both groups were similar in age. The patients with

Published OnlineFirst September 27, 2011; DOI:10.1158/1940-6207.CAPR-11-0096

Table 2. Logistic-regression models fitted on the training set to screen for SCC at the upper aerodigestive tract based on traditional risk factors or epigenetic markers

	Univariate analyses			Multivariate analyses with model selection		
Risk factors	**Crude OR**	**95% CI**	***P***	**Adjusted OR**	**95% CI**	***P***
Models based on the traditional risk factors						
Age	1.009	0.990–1.028	0.357			
Male sex	5.405	2.515–11.618	<0.001			
BMI	0.935	0.875–0.998	0.042			
Lifestyle risk factors						
Levels of alcohol drinking	1.199	1.148–1.252	<0.001			
Levels of betel quid chewing	1.131	1.080–1.185	<0.001			
Levels of cigarette smoking	1.176	1.122–1.233	<0.001			
Any one of the above	10.533	5.766–19.239	<0.001	4.172	1.515–11.488	0.006
Genetic polymorphisms						
*ALDH2*1/2*2* or *2*2/2*2*, slow	1.563	0.841–2.904	0.158			
*ADH1B*1/*1*, slow	1.904	0.881–4.115	0.101			
*ADH1C*1/*1*, fast	0.437	0.165–1.161	0.097			
GSTP1 ile/ile, slow	1.923	0.767–4.817	0.163			
GSTM1 null, inactive	0.822	0.434–1.559	0.549			
GSTT1 null, inactive	0.943	0.502–1.773	0.856			
MCV	1.061	1.011–1.114	0.015	1.060	1.000–1.124	0.049
H. pylori infection	1.553	0.927–2.601	0.094			
Human papillomavirus infection	1.487	0.598–3.696	0.391			
Presence of numerous LVLs in the background mucosae	14.965	6.176–36.263	<0.001	9.384	3.058–28.795	<0.001
Models based on the epigenetic markers						
HOXA9 methylation level (%)	1.153	1.101–1.209	<0.001	1.141	1.086–1.198	<0.001
NEFH methylation level (%)	1.670	1.280–2.179	<0.001	1.339	1.078–1.664	0.008
UCHL1 methylation level (%)	1.199	1.069–1.345	0.002			
MT1M methylation level (%)	1.474	1.153–1.884	0.002			

SCC tended to be male, lower in BMI, and more likely to have the ABC habits. Serologically, their MCVs were higher, but their rate of *H. pylori* and human papillomavirus infections was similar to that of the controls. Endoscopy found that the cancer patients were more likely to have numerous LVLs in the background mucosae. A significant interaction was found between carriers of the genetic polymorphisms of an inactive *ALDH2*2* allele and levels of alcohol consumption (OR: 1.212, 95% CI: 1.092–1.344, $P < 0.001$), as observed in the Hardy–Weinberg equilibrium, indicating that this genotype modified alcohol-related cancer risk.

Model performance was compared in terms of ROC curves (Supplementary Fig. S11). Overall exposure to ABC had a higher sensitivity (93%, 95% CI: 90%–96%) but a lower specificity (45%, 95% CI: 35%–54%), while the presence of endoscopic LVLs had a lower sensitivity (50%, 95% CI: 44%–56%) but a higher specificity (92%, 95% CI: 88%–98%). The AUCs increased as the model was based on MCV; then that based on overall exposure to ABC, endoscopic LVLs, and MCV (the traditional model; goodness-of-fit test, $P = 0.77$); then that based on methylation levels of *HOXA9* and *NEFH* (the epigenetic model; goodness-of-fit test, $P = 0.18$); and then that based on the overall exposure to ABC, endoscopic LVLs, and methylation levels of *HOXA9* and *NEFH* (the combined model shown in Table 3; goodness-of-fit test, $P = 0.70$), which was the most accurate. The sensitivity and specificity pairs of the optimal cutpoints were 56% (95% CI: 48%–64%) and 57% (48%–66%) for the MCV-based model, 74% (67%–81%) and 74% (66%–82%) for the traditional model, 74% (69%–79%) and 75% (67%–83%) for the epigenetic model, and 82% (76%–88%) and 81% (74%–88%) for the combined model. The performance of epigenetic model (AUC: 83%, bootstrap 95% CI: 79%–87%) was similar to that of the traditional model (AUC: 80%, 95% CI: 67%–91%; $P = 0.51$ for the comparison). After adding the epigenetic markers, the combined model (AUC: 91%, 95% CI: 88%–94%) was more accurate than the traditional model ($P < 0.001$).

Comparing performance between training and validation sets

Between May 2009 and May 2011, a total of 224 patients who underwent endoscopic screening were recruited as the validation set. They included 74 with negative endoscopies,

Published OnlineFirst September 27, 2011; DOI:10.1158/1940-6207.CAPR-11-0096

Table 3. Logistic-regression models fitted on the training set to screen for SCC at the upper aerodigestive tract based on the combination of traditional risk factors and epigenetic markers

	Multivariate analyses with model selection		
Risk factors	**Adjusted OR**	**95% CI**	***P***
Models based on both traditional risk factors and epigenetic markers			
Exposure to at least one of ABC	4.557	1.141–18.208	0.032
Presence of numerous LVLs in the background mucosae	8.428	2.458–28.903	<0.001
HOXA9 methylation level (%)	1.118	1.039–1.204	0.003
NEFH methylation level (%)	1.350	1.042–1.749	0.023

86 with head and neck cancer (6 with oral cavity cancer, 6 with oropharyngeal cancer, 5 with laryngeal cancer, and 69 with hypopharyngeal cancer), 59 with esophageal cancer, and 5 patients with synchronous head and neck and esophageal cancers. Their distribution of age (58.2 ± 12.5 y), gender (86.6% men), BMI (22.2 ± 3.7 kg/m^2), and exposure to ABC (80.4%) was similar to that of the original training cohort. Methylation levels of the 4 markers in the normal esophageal mucosae of the control group were 2.9% ± 2.9% (average ± SD; median: 1.8%; range: 0%–12.4%) for *HOXA9*, 0.4% ± 0.7% (0.1%; 0%–6%) for *NEFH*, 0.5% ± 0.7% (0.1%; 0%–3.2%) for *UCHL1*, and 0.2% ± 0.5% (0.1%; 0%–3.4%) for *MT1M*. The normal esophageal mucosae of the cancer group had methylation levels of 13.5% ± 16.8% (5.9%; 0.1%–84.6%) for *HOXA9*, 1.1% ± 4.2% (0.2%; 0%–47.6%) for *NEFH*, 3.8% ± 11.7% (0.6%; 0%–82.0%) for *UCHL1*, and 2.4% ± 10.2% (0.2%; 0%–92.3%) for *MT1M*. When the epigenetic model fit in the training set was applied to the validation set, the AUC was 80% (bootstrap 95% CI: 73%–85%; goodness-of-fit test, $P = 0.16$); the difference in discrimination between the training and validation sets was not statistically significant ($P = 0.43$; Fig. 2). The *HOXA9* remained the best discriminative marker with 78% AUC (95% CI: 72%–84%) in predicting UADT cancer.

Discussion

Our present study quantified use of epigenetics for cancerization with small diagnostic biopsies from normal esophageal mucosae. We confirmed that this approach is equivalent to the traditional risk factor method, which typically requires a comprehensive set of clinical data. The biological significance of the epigenetic approach is supported by studies investigating the pathogenesis of SCC, which find that *HOXA9* protein expression is deregulated in SCC (32), that oncogenesis is triggered by silencing *NEFH* to activate the Akt/β-catenin pathway (33), that the prognosis of SCC is worsened by hypermethylating *UCHL1* (34) that interacts with *p53* through the deubiquitination pathway (35), and that overexpressing *MT* is associated with metastatic and proliferative activity (36). None of these 4 genes had previously been correlated with carcinogen exposure or with cancer risk prediction.

Our study provided abundant information regarding the effects of traditional risk factors. As expected, ABCs were strong determinants that led to a lower BMI and a higher MCV, indicating poor nutritional status (7). However, judgment-based merely on the overall exposure to ABC was insufficient because the false-positive rate (55%) was high. Both of the infectious pathogens *H. pylori* and human papillomavirus were not associated with SCC risk (37, 38). Although several risk alleles have been previously identified (10–13), they served as effect modifiers rather than direct causes. Although the value of endoscopic LVLs has been confirmed, the usefulness of Lugol staining as a first-line screening tool is limited by a lower sensitivity (50%), in addition to significant side effects. A substantial proportion of subjects with cancer risk would be lost from surveillance if the risk assessment was solely based on the presence of endoscopic LVLs. However, the above limitations of traditional risk factors might support the credibility of our findings since our findings are similar to other literature reports (summarized in the Supplementary Table S2; refs. 15, 19, 20).

Taking into consideration both measured and unmeasured risk factors/genetic susceptibilities, molecular information derived from histologically normal mucosae has been extensively investigated, such as the field effects of oral leukoplakia, Barrett's esophagus (39), and colon neoplasm (40, 41). Mutations of *p53* or *p53* oncoprotein are relatively late events in carcinogenesis (42, 43), so, despite their biological plausibility as cancer predictors, they are insufficient for risk assessments for SCC in the UADT. Because aberrant DNA methylation usually precedes neoplastic transformation, qualitative studies have suggested that the presence of methylated genes may increase in a sequence from normal mucosa to precursor lesions to SCC (44–46). Our study further found that this phenomenon is quantitative for individual gene markers.

Research on clinical applications found that a candidate gene approach measuring the methylation of *AHRR*, *p16INK4a*, *MT1G*, and *CLDN3* had unsatisfactory sensitivity of 50% and specificity value of 68% when screening for SCC in China with esophageal-balloon cytology (47). In contrast, the performance of our 4-gene panel may effectively identify subjects who will benefit from endoscopic surveillance. Our panel's superiority may be due to our

Published OnlineFirst September 27, 2011; DOI:10.1158/1940-6207.CAPR-11-0096

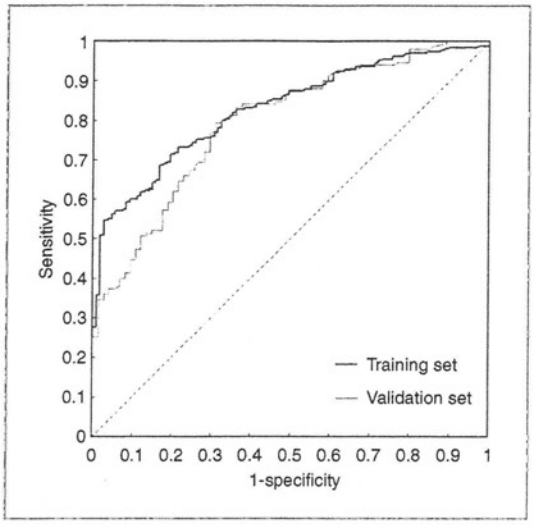

Figure 2. ROC curve shows the prediction of upper aerodigestive tract cancer with epigenetic markers in the training and validation sets. The area under the ROC curve was 83% (bootstrap 95% CI: 79%–87%) in the training set and 80% (bootstrap 95% CI: 73%–85%) in the validation set (training vs. validation ROC, $P = 0.43$). The dashed line represents a test of no discrimination.

meticulous search for candidate genes by oligonucleotide microarray, which decreased bias in choosing targets (30), and to using qMSP to extract full information without truncating the methylation value (23). Imaging-enhanced endoscopies minimized the risk of contamination during sample collection (28, 29). The similar methylation patterns between the 2 ethnically different populations from Japan and Taiwan further strengthens the generalizability of our approach. Our approach is accurate, inexpensive with the cost estimated at one USD per specimen marker, and high throughput. This can allow surveillance with sophisticated technologies to focus on high-risk patients, which is potentially cost effective.

Intriguingly, the *HOXA9* gene, which is essential for embryogenesis and organogenesis, was identified as the most informative marker. This finding underscored the significance of *HOX* genes in regulating cell proliferation and differentiation, which is a balance that shifts in tumorigenesis (48). Also noteworthy are the contributions of overall exposure to ABC and of endoscopic LVLs, which remained significant in the combined model that yielded the highest AUC of 91%. This result may partially reflect the design of our screening procedure on the basis of alcohol and cigarette use (30) rather than on betel quid chewing. Betel quid chewing is a well-recognized class-1 carcinogen, so residual confounding cannot be ruled out. Recruiting more patients with heavy exposure to betel quid would be worthwhile because markers tailored to this substance could be identified by methylated DNA immunoprecipitation microarray (49).

Our risk-assessment models predicted the risk of actually finding SCC at the endoscopy when the biopsies were taken. The results may need to be verified by longitudinal data following the development of aberrant methylation in those with ongoing exposure to carcinogens. This would allow us to elucidate how many individuals with positive methylation markers would eventually go on to develop SCC (50). Individuals with normal mucosae, low methylation levels, and exposure to carcinogens may also benefit from risk stratification by modifying lifestyle risk factors to reduce cancer risk. In addition, although similar etiologic factors are involved in the development of head and neck cancer and esophageal cancer, they are not created equally. Our patients with head and neck cancer were mainly composed of those with hypopharyngeal cancer, so our results may not be so readily applied to those with oral cavity cancer. Therefore, this topic warrants further investigation.

In conclusion, we successfully quantified the field for cancerization using epigenetic markers. Our work provides a better model for risk assessment and may potentially be generalized across the high-risk regions to allocate the limited endoscopic resources for the surveillance and early detection of UADT cancers.

Disclosure of Potential Conflicts of Interest

No potential conflicts of interest were disclosed.

Acknowledgments

The authors thank Luan-Yin Chang, MD, PhD, Department of Pediatrics, College of Medicine, National Taiwan University, for helping to determine the cutoff point to positively determine human papillomavirus infection.

Grant Support

This study was supported by research grants from the National Science Council (NSC96-2314-B-002-092-MY3) and the Taipei Institute of Pathology.

The costs of publication of this article were defrayed in part by the payment of page charges. This article must therefore be hereby marked *advertisement* in accordance with 18 U.S.C. Section 1734 solely to indicate this fact.

Received February 22, 2011; revised July 15, 2011; accepted August 31, 2011; published OnlineFirst September 27, 2011.

References

1. Boyle P, Levin B. World cancer report. Lyon, France: IARC press; 2008.
2. Muto M, Minashi K, Yano T, Saito Y, Oda I, Nonaka S, et al. Early detection of superficial squamous cell carcinoma in the head and neck region and esophagus by narrow band imaging: a multicenter randomized controlled trial. J Clin Oncol 2010;28:1566–72.
3. Yen AM, Chiu YH, Chen LS, Wu HM, Huang CC, Boucher BJ, et al. A population-based study of the association between betel-quid chewing and the metabolic syndrome in men. Am J Clin Nutr 2006; 83:1153–60.
4. National Department of Health, Taiwan, Republic of China. Cancer Registry Annual Report 1972–2009.
5. Wei WQ, Abnet CC, Lu N, Roth MJ, Wang GQ, Dye BA, et al. Risk factors for oesophageal squamous dysplasia in adult inhabitants of a high risk region of China. Gut 2005;54:759–63.

Published OnlineFirst September 27, 2011; DOI:10.1158/1940-6207.CAPR-11-0096

6. Wang WL, Lee CT, Lee YC, Hwang TZ, Wang CC, Hwang JC, et al. Risk factors for developing synchronous esophageal neoplasia in patients with head and neck cancer. Head Neck 2011;33:77–81.
7. Park SL, Lee YC, Marron M, Agudo A, Ahrens W, Barzan L, et al. The association between change in body mass index and upper aerodigestive tract cancers in the ARCAGE project: Multicenter case-control study. Int J Cancer 2011;128:1449–61.
8. Lee CH, Lee JM, Wu DC, Hsu HK, Kao EL, Huang HL, et al. Independent and combined effects of alcohol intake, tobacco smoking and betel quid chewing on the risk of esophageal cancer in Taiwan. Int J Cancer 2005;113:475–82.
9. Ishiguro S, Sasazuki S, Inoue M, Kurahashi N, Iwasaki M, Tsugane S. JPHC Study Group. Effect of alcohol consumption, cigarette smoking and flushing response on esophageal cancer risk: a population-based cohort study (JPHC study). Cancer Lett 2009;275:240–6.
10. Brennan P, Lewis S, Hashibe M, Bell DA, Boffetta P, Bouchardy C, et al. Pooled analysis of alcohol dehydrogenase genotypes and head and neck cancer: a HuGE review. Am J Epidemiol 2004;159:1–16.
11. Lee CH, Lee JM, Wu DC, Goan YG, Chou SH, Wu IC, et al. Carcinogenetic impact of ADH1B and ALDH2 genes on squamous cell carcinoma risk of the esophagus with regard to the consumption of alcohol, tobacco and betel quid. Int J Cancer 2008;122:1347–56.
12. Cui R, Kamatani Y, Takahashi A, Usami M, Hosono N, Kawaguchi T, et al. Functional variants in ADH1B and ALDH2 coupled with alcohol and smoking synergistically enhance esophageal cancer risk. Gastroenterology 2009;137:1768–75.
13. Tanaka F, Yamamoto K, Suzuki S, Inoue H, Tsurumaru M, Kajiyama Y, et al. Strong interaction between the effects of alcohol consumption and smoking on oesophageal squamous cell carcinoma among individuals with ADH1B and/or ALDH2 risk alleles. Gut 2010;59:1457–64.
14. Lee JM, Lee YC, Yang SY, Shi WL, Lee CJ, Luh SP, et al. Genetic polymorphisms of p53 and GSTP1, but not NAT2, are associated with susceptibility to squamous-cell carcinoma of the esophagus. Int J Cancer 2000;89:458–64.
15. Yokoyama A, Yokoyama T, Muramatsu T, Omori T, Matsushita S, Higuchi S, et al. Macrocytosis, a new predictor for esophageal squamous cell carcinoma in Japanese alcoholic men. Carcinogenesis 2003;24:1773–8.
16. Wu DC, Wu IC, Lee JM, Hsu HK, Kao EL, Chou SH, et al. Helicobacter pylori infection: a protective factor for esophageal squamous cell carcinoma in a Taiwanese population. Am J Gastroenterol 2005;100:588–93.
17. Whiteman DC, Parmar P, Fahey P, Moore SP, Stark M, Zhao ZZ, et al. Australian Cancer Study. Association of Helicobacter pylori infection with reduced risk for esophageal cancer is independent of environmental and genetic modifiers. Gastroenterology 2010;139:73–83.
18. D'Souza G, Kreimer AR, Viscidi R, Pawlita M, Fakhry C, Koch WM, et al. Case-control study of human papillomavirus and oropharyngeal cancer. N Engl J Med 2007;356:1944–56.
19. Muto M, Hironaka S, Nakane M, Boku N, Ohtsu A, Yoshida S. Association of multiple Lugol-voiding lesions with synchronous and metachronous esophageal squamous cell carcinoma in patients with head and neck cancer. Gastrointest Endosc 2002;56:517–21.
20. Yokoyama T, Yokoyama A, Kumagai Y, Omori T, Kato H, Igaki H, et al. Health risk appraisal models for mass screening of esophageal cancer in Japanese men. Cancer Epidemiol Biomarkers Prev 2008;17:2846–54.
21. Muto M, Nakane M, Hitomi Y, Yoshida S, Sasaki S, Ohtsu A, et al. Association between aldehyde dehydrogenase gene polymorphisms and the phenomenon of field cancerization in patients with head and neck cancer. Carcinogenesis 2002;23:1759–65.
22. Taby R, Issa JP. Cancer epigenetics. CA Cancer J Clin 2010;60:376–92.
23. Nakajima T, Enomoto S, Ushijima T. DNA methylation: a marker for carcinogen exposure and cancer risk. Environ Health Prev Med 2008;13:8–15.
24. Mehanna H, Paleri V, West CM, Nutting C. Head and neck cancer–Part 1: Epidemiology, presentation, and prevention. BMJ 2010;341:c4684.
25. Chung CS, Lee YC, Wang CP, Ko JY, Wang WL, Wu MS, et al. Secondary prevention of esophageal squamous cell carcinoma in areas where smoking, alcohol, and betel quid chewing are prevalent. J Formos Med Assoc 2010;109:408–21.
26. Liou JM, Lin JT, Wang HP, Huang SP, Lee YC, Chiu HM, et al. IL-1B-511 C–>T polymorphism is associated with increased host susceptibility to Helicobacter pylori infection in Chinese. Helicobacter 2007;12:142–9.
27. Chen CJ, Viscidi RP, Chuang CH, Huang YC, Chiu CH, Lin TY. Seroprevalence of human papillomavirus types 16 and 18 in the general population in Taiwan: implication for optimal age of human papillomavirus vaccination. J Clin Virol 2007;38:126–30.
28. Lee YC, Wang CP, Chen CC, Chiu HM, Ko JY, Lou PJ, et al. Transnasal endoscopy with narrow-band imaging and Lugol staining to screen patients with head and neck cancer whose condition limits oral intubation with standard endoscope (with video). Gastrointest Endosc 2009;69:408–17.
29. Wang CP, Lee YC, Yang TL, Lou PJ, Ko JY. Application of unsedated transnasal esophagogastroduodenoscopy in the diagnosis of hypopharyngeal cancer. Head Neck 2009;31:153–7.
30. Oka D, Yamashita S, Tomioka T, Nakanishi Y, Kato H, Kaminishi M, et al. The presence of aberrant DNA methylation in noncancerous esophageal mucosae in association with smoking history: a target for risk diagnosis and prevention of esophageal cancers. Cancer 2009;115:3412–26.
31. Gönen M. Comparison and covariate adjustment of ROC curves. In: Gönen M, editor. Analyzing receiver operating characteristic curves with SAS. Cary, NC: SAS Institute Inc.; 2007. p. 37–52.
32. Chen KN, Gu ZD, Ke Y, Li JY, Shi XT, Xu GW. Expression of 11 HOX genes is deregulated in esophageal squamous cell carcinoma. Clin Cancer Res 2005;11:1044–9.
33. Kim MS, Chang X, LeBron C, Nagpal JK, Lee J, Huang Y, et al. Neurofilament heavy polypeptide regulates the Akt-beta-catenin pathway in human esophageal squamous cell carcinoma. PLoS One 2010;5:e9003.
34. Mandelker DL, Yamashita K, Tokumaru Y, Mimori K, Howard DL, Tanaka Y, et al. PGP9.5 promoter methylation is an independent prognostic factor for esophageal squamous cell carcinoma. Cancer Res 2005;65:4963–8.
35. Yu J, Tao Q, Cheung KF, Jin H, Poon FF, Wang X, et al. Epigenetic identification of ubiquitin carboxyl-terminal hydrolase L1 as a functional tumor suppressor and biomarker for hepatocellular carcinoma and other digestive tumors. Hepatology 2008;48:508–18.
36. Hishikawa Y, Koji T, Dhar DK, Kinugasa S, Yamaguchi M, Nagasue N. Metallothionein expression correlates with metastatic and proliferative potential in squamous cell carcinoma of the oesophagus. Br J Cancer 1999;81:712–20.
37. Rokkas T, Pistiolas D, Sechopoulos P, Robotis I, Margantinis G. Relationship between Helicobacter pylori infection and esophageal neoplasia: a meta-analysis. Clin Gastroenterol Hepatol 2007;5:1413–7, 1417.e1–2.
38. Koshiol J, Wei WQ, Kreimer AR, Chen W, Gravitt P, Ren JS, et al. No role for human papillomavirus in esophageal squamous cell carcinoma in China. Int J Cancer 2010;127:93–100.
39. Reid BJ. Cancer risk assessment and cancer prevention: promises and challenges. Cancer Prev Res 2008;1:229–32.
40. Paun BC, Kukuruga D, Jin Z, Mori Y, Cheng Y, Duncan M, et al. Relation between normal rectal methylation, smoking status, and the presence or absence of colorectal adenomas. Cancer 2010;116:4495–501.
41. Wallace K, Grau MV, Levine AJ, Shen L, Hamdan R, Chen X, et al. Association between folate levels and CpG island hypermethylation in normal colorectal mucosa. Cancer Prev Res 2010;3:1552–64.
42. Roth MJ, Hu N, Emmert-Buck MR, Wang QH, Dawsey SM, Li G, et al. Genetic progression and heterogeneity associated with the development of esophageal squamous cell carcinoma. Cancer Res 2001;61:4098–104.
43. van Houten VM, Tabor MP, van den Brekel MW, Kummer JA, Denkers F, Dijkstra J, et al. Mutated p53 as a molecular marker for the diagnosis of head and neck cancer. J Pathol 2002;198:476–86.
44. Roth MJ, Abnet CC, Hu N, Wang QH, Wei WQ, Green L, et al. p16, MGMT, RARbeta2, CLDN3, CRBP and MT1G gene methylation in esophageal squamous cell carcinoma and its precursor lesions. Oncol Rep 2006;15:1591–7.

Published OnlineFirst September 27, 2011; DOI:10.1158/1940-6207.CAPR-11-0096

45. Guo M, Ren J, House MG, Qi Y, Brock MV, Herman JG. Accumulation of promoter methylation suggests epigenetic progression in squamous cell carcinoma of the esophagus. Clin Cancer Res 2006;12:4515–22.
46. Ishii T, Murakami J, Notohara K, Cullings HM, Sasamoto H, Kambara T, et al. Oesophageal squamous cell carcinoma may develop within a background of accumulating DNA methylation in normal and dysplastic mucosa. Gut 2007;56:13–9.
47. Adams L, Roth MJ, Abnet CC, Dawsey SP, Qiao YL, Wang GQ, et al. Promoter methylation in cytology specimens as an early detection marker for esophageal squamous dysplasia and early esophageal squamous cell carcinoma. Cancer Prev Res 2008;1:357–61.
48. Chen H, Sukumar S. HOX genes: emerging stars in cancer. Cancer Biol Ther 2003;2:524–5.
49. Yamashita S, Hosoya K, Gyobu K, Takeshima H, Ushijima T. Development of a novel output value for quantitative assessment in methylated DNA immunoprecipitation-CpG island microarray analysis. DNA Re 2009;16:275–86.
50. Ulrich CM, Grady WM. Linking epidemiology to epigenomics–where are we today? Cancer Prev Res 2010;3:1505–8.

Oncogene (2011) 1–12

www.nature.com/onc

ORIGINAL ARTICLE

Inflammation-induced repression of tumor suppressor miR-7 in gastric tumor cells

D Kong[1,7], Y-S Piao[1,7,8], S Yamashita[2], H Oshima[1], K Oguma[1], S Fushida[3], T Fujimura[3], T Minamoto[4], H Seno[5], Y Yamada[6], K Satou[6], T Ushijima[2], T-O Ishikawa[1] and M Oshima[1]

[1]Division of Genetics, Cancer Research Institute, Kanazawa University, Kanazawa, Japan; [2]Division of Epigenomics, National Cancer Center Research Institute, Tokyo, Japan; [3]Department of Gastroenterologic Surgery, Kanazawa University Hospital, Kanazawa, Japan; [4]Division of Translational and Clinical Oncology, Cancer Research Institute, Kanazawa University, Kanazawa, Japan; [5]Department of Gastroenterology and Hepatology, Kyoto University Graduate School of Medicine, Kyoto, Japan and [6]Faculty of Electrical and Computer Engineering, Institute of Science and Engineering, Kanazawa University, Kanazawa, Japan

Inflammation has an important role in cancer development through various mechanisms. It has been shown that dysregulation of microRNAs (miRNAs) that function as oncogenes or tumor suppressors contributes to tumorigenesis. However, the relationship between inflammation and cancer-related miRNA expression in tumorigenesis has not yet been fully understood. Using *K19-C2mE* and *Gan* mouse models that develop gastritis and gastritis-associated tumors, respectively, we found that 21 miRNAs were upregulated, and that 29 miRNAs were downregulated in gastric tumors in an inflammation-dependent manner. Among these miRNAs, the expression of miR-7, a possible tumor suppressor, significantly decreased in both gastritis and gastric tumors. Moreover, the expression of miR-7 in human gastric cancer was inversely correlated with the levels of interleukin-1β and tumor necrosis factor-α, suggesting that miR-7 downregulation is related to the severity of inflammatory responses. In the normal mouse stomach, miR-7 expression was at a basal level in undifferentiated gastric epithelial cells, and was induced during differentiation. Moreover, transfection of a miR-7 precursor into gastric cancer cells suppressed cell proliferation and soft agar colony formation. These results suggest that suppression of miR-7 expression is important for maintaining the undifferentiated status of gastric epithelial cells, and thus contributes to gastric tumorigenesis. Although epigenetic changes were not found in the CpG islands around miR-7-1 of gastritis and gastric tumor cells, we found that activated macrophage-derived small molecule(s) (<3 kDa) are responsible for miR-7 repression in gastric cancer cells. Furthermore, the miR-7 expression level significantly decreased in the inflamed gastric mucosa of *Helicobacter*-infected mice, whereas it increased in the stomach of germfree *K19-C2mE* and *Gan* mice wherein inflammatory responses were suppressed. Taken together, these results indicate that downregulation of tumor suppressor miR-7 is a novel mechanism by which the inflammatory response promotes gastric tumorigenesis.

Oncogene advance online publication, 5 December 2011; doi:10.1038/onc.2011.558

Keywords: miR-7; gastric cancer; inflammation; macrophages

Introduction

It has been established that inflammatory responses contribute to cancer development through various mechanisms (Coussens and Werb, 2002). The expression of cyclooxygenase-2 (COX-2), a rate-limiting enzyme for prostaglandin biosynthesis, has an important role in both inflammation and cancer (Wang and DuBois, 2010). Using genetic mouse models, we previously demonstrated that induction of COX-2 and its downstream product, prostaglandin E_2 (PGE_2), is required for gastrointestinal tumorigenesis (Sonoshita *et al.*, 2001; Oshima *et al.*, 2006). The COX-2/PGE_2 pathway, together with a bacterial infection, induces inflammatory responses in the stomach through the recruitment of macrophages, which promotes gastric tumorigenesis (Oshima *et al.*, 2011). However, it remains to be fully elucidated precisely how such inflammatory responses contribute to the promotion of gastric tumors.

MicroRNAs (miRNAs) are a class of single-stranded small noncoding RNAs that regulate gene expression by post-transcriptional interference of specific mRNAs (Ambros, 2004; Bartel, 2004). Through their regulation of cancer-related gene expression, miRNAs can function as either oncogenes or tumor suppressors (Esquela-Kerscher and Slack, 2006; Ventura and Jacks, 2009). Dysregulation of miRNAs in cancer has been shown to be associated with genomic/epigenetic alterations or transcriptional/post-transcriptional mechanisms (Di Leva and Croce, 2010). Moreover, expression of several miRNAs, including oncogenic miRNAs, has been shown to be induced by inflammatory

Correspondence: Professor M Oshima, Division of Genetics, Cancer Research Institute, Kanazawa University, Kakuma-machi, Kanazawa, 920-1192, Japan.
E-mail: oshimam@kenroku.kanazawa-u.ac.jp
[7]These authors contributed equally to this work.
[8]Current address: Department of Pathophysiology, Medical College, Yanbian University, Yanji City 133002, China.
Received 18 July 2011; revised 22 October 2011; accepted 2 November 2011

responses (Sonkoly and Pivarcsi, 2011). For example, miR-155 is induced in macrophages by nuclear factor-κB, interferon-β or Toll-like receptor signaling (O'Connell *et al.*, 2007; Tili *et al.*, 2007), whereas miR-21 is induced by Stat3, a transcription factor activated by interleukin-6 (IL-6) (Iliopoulos *et al.*, 2010). On the other hand, the mechanism responsible for the downregulation of tumor-suppressor miRNA expression in the inflammatory microenvironment has not been fully understood.

Herein, we examined the expression of miRNAs in mouse models of gastritis and gastric tumors, which were developed in *K19-C2mE* and *Gan* mice, respectively (Oshima *et al.*, 2004, 2006). We found the expression level of miR-7 to significantly decrease in gastric tumors in an inflammation-dependent manner. It has been shown that miR-7 has a tumor-suppressor role in several cancers, including glioblastoma, breast cancer and lung cancer (Kefas *et al.*, 2008; Reddy *et al.*, 2008; Webster *et al.*, 2009; Jiang *et al.*, 2010; Saydam *et al.*, 2011). In this manuscript, we demonstrate that miR-7 is induced during the differentiation of normal gastric epithelial cells, and it also has a tumor-suppressor role in the stomach. These results suggest that downregulation of tumor suppressor miR-7 is one of the tumor-promoting mechanisms underlying the role of inflammation in gastric tumorigenesis.

Results

Inflammation-dependent dysregulation of miRNAs in gastric tumors

To examine whether miRNA expression is dysregulated in gastric tumors by inflammatory responses, we examined the miRNA expression profiles in wild-type mouse stomachs, *K19-C2mE* mouse gastritis and *Gan* mouse gastric tumors by a microarray analysis. In *Gan* mouse gastric tumors, 50 miRNAs were upregulated (>2.0-fold), whereas 42 miRNAs were downregulated (<0.5-fold) compared with the wild-type mouse stomach level (Figure 1a and Supplementary Table 1). Notably, 21 and 29 miRNAs showed upregulation or downregulation, respectively, in both gastritis and gastric tumors. Therefore, it is possible that dysregulation of these miRNAs is caused by inflammatory responses.

We confirmed the results of the microarray analysis by real-time reverse transcriptase–polymerase chain reaction (RT–PCR). In all, 10 miRNAs randomly selected from the upregulated and downregulated miRNAs (Figure 1a, boxed) showed the same dysregulation pattern in both gastritis and gastric tumors (Figure 1b). Importantly, miR-155 and miR-21, which function as oncogenes (Volinia *et al.*, 2006) were upregulated, whereas miR-145 and miR-7, which function as tumor suppressors (Kefas *et al.*, 2008; Sachdeva *et al.*, 2009), were downregulated in both gastritis and gastric tumors (Figures 1a and b). This suggests that inflammation can induce not only upregulation of oncogenic miRNAs but also downregulation of tumor-suppressor miRNAs.

We next picked up 74 miRNAs that were not dysregulated in *K19-C2mE* gastritis compared with the wild-type normal stomach (Supplementary Table 2). Among them, three miRNAs were upregulated in *Gan* mouse tumors compared with *K19-C2mE* gastritis tissue samples (>2.0-fold), whereas three miRNA were downregulated (<0.5-fold) (Figure 1c). It is possible that expression of these miRNAs is dysregulated by carcinogenesis-specific mechanisms.

Induction of miR-7 during differentiation of gastric epithelial cells

We further examined the expression of miR-7, because its role(s) in the normal stomach and gastric cancer have never been examined. Gastric glands were isolated from the stomachs of the respective mouse models, and the miR-7 expression was examined by real-time RT–PCR. Notably, miR-7 levels were significantly lower in epithelial cells of *K19-C2mE* gastritis tissues and *Gan* mouse tumors compared with the wild-type mouse stomach (Figure 2a), indicating that miR-7 is predominantly expressed in epithelial cells in an inflammation-dependent manner.

When primary cultured gastric epithelial cells were passaged and maintained for 6 days, the cell morphology appeared to be differentiated, with enlarged and mucin-containing cytoplasm (Figure 2b). Consistently, the expression of differentiation markers, *Muc6* and *Muc5AC*, was elevated on day 6, whereas the expression of the Wnt target gene, *Sox9*, decreased (Figure 2c). These results indicate that cultured gastric epithelial cells underwent differentiation through passage and 6-day culture. Importantly, the miR-7 expression level increased significantly on day 6 to 6.5-fold, compared with the level observed on day 2.

We next examined the miR-7 level in the stomach during development. The expression level of miR-7 in the stomach increased significantly in 14-day-old and adult mice, to >6-fold of that in E15 embryos (Figure 2d). Conversely, expression of *CD44*, one of the Wnt target genes, decreased significantly during development. We confirmed by an immunohistochemistry that most epithelial cells in the gastric mucosa were Ki-67 positive on days 0 and 7, whereas proliferating cells were limited to the gland neck on day 14 and in adult mice (Figure 2e). Accordingly, the ratio of undifferentiated epithelial cells decreased during development. Taken together, these results indicate that miR-7 expression is induced in gastric epithelial cells during differentiation.

Tumor-suppressor role of miR-7 in gastric cancer development

We next examined miR-7 levels in human gastric cancers by real-time RT–PCR. The expression of miR-7 was downregulated in 18 out of 28 human gastric cancer tissue samples (64%) compared with paired non-tumor stomach tissue samples (Figure 3a), suggesting that miR-7 has a tumor-suppressor role in a subpopulation of gastric cancers. We next examined the expression

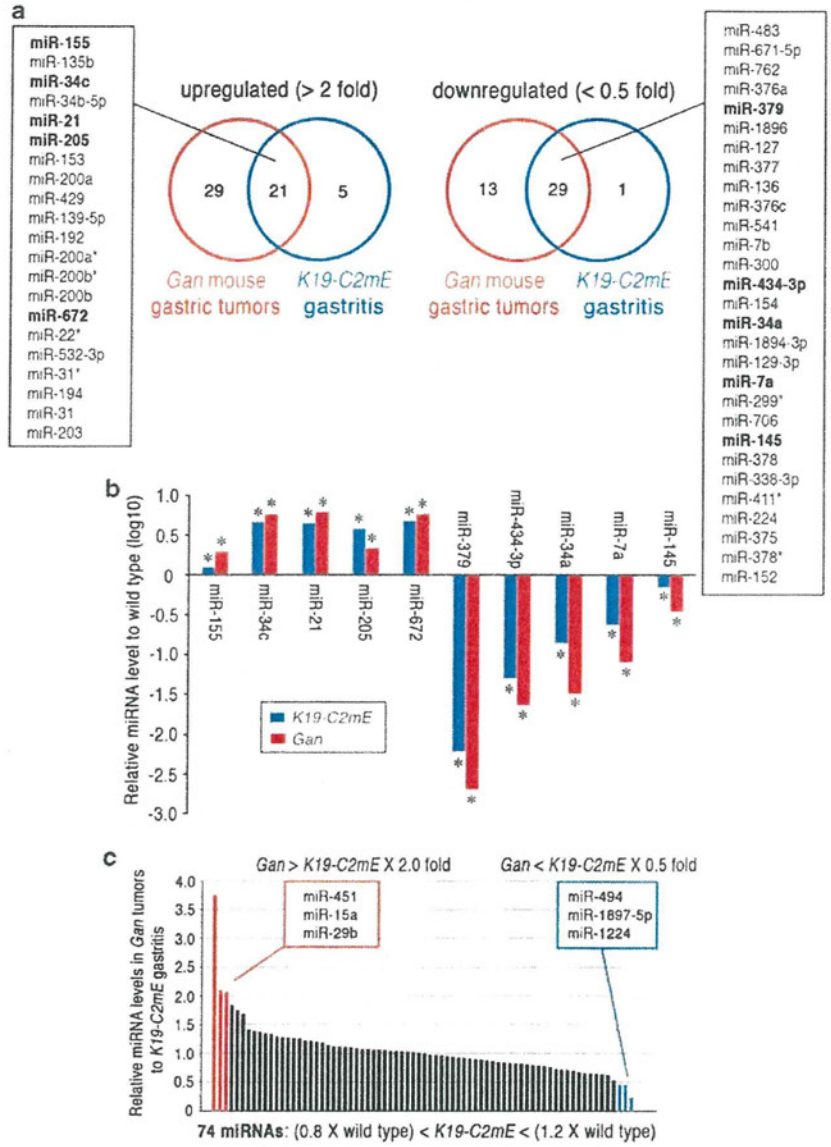

Figure 1 Inflammation-dependent dysregulation of miRNA expression in mouse gastric tumors. (**a**) Venn diagrams of the miRNAs that were upregulated (>2.0) and downregulated (<0.5) in *Gan* mouse gastric tumors and/or *K19-C2mE* mouse gastritis samples as determined by the microarray analysis are shown. The miRNAs listed in boxes were upregulated (left) or downregulated (right) in both gastric tumor and gastritis tissue samples. (**b**) The relative expression levels of selected miRNAs (indicated in bold in the list) for *K19-C2mE* mouse gastritis (blue bars) and *Gan* mouse gastric tumors (red bars) compared with the wild-type levels examined by real-time RT–PCR are shown as the log10 ratios. *$P<0.05$ versus the wild-type level. The expression levels of miRNAs were normalized to the Sno202 level. (**c**) The miRNA levels in *Gan* mouse tumors relative to those in *K19-C2mE* gastritis tissues examined by the microarray analysis are shown. Red and blue bars indicate upregulated (>2.0) and downregulated (<0.5) miRNAs, respectively, in *Gan* mouse tumors.

level of IL-1β and tumor necrosis factor (TNF)-α, major proinflammatory cytokines, and compared them with the miR-7 level. Importantly, expression levels of miR-7 were inversely correlated with those of IL-1β or TNF-α, suggesting that the downregulation of miR-7 is related to the severity of inflammatory responses (Figure 3b). We also found that miR-7 was markedly downregulated in four out of nine gastric cancer cells lines (Figure 3c).

To examine the tumor-suppressor role of miR-7 in gastric tumorigenesis, we transfected the precursor of miR-7, pre-miR-7, into AZ-521 and Kato-III gastric cancer cells and examined their proliferation and soft agar colony formation. We confirmed that pre-miR-7 transfection into reporter vector-transfected cells resulted in a significant decrease in luciferase activity, indicating an increase of mature miR-7 level (Supplementary Figure 1). Transfection of pre-miR-7

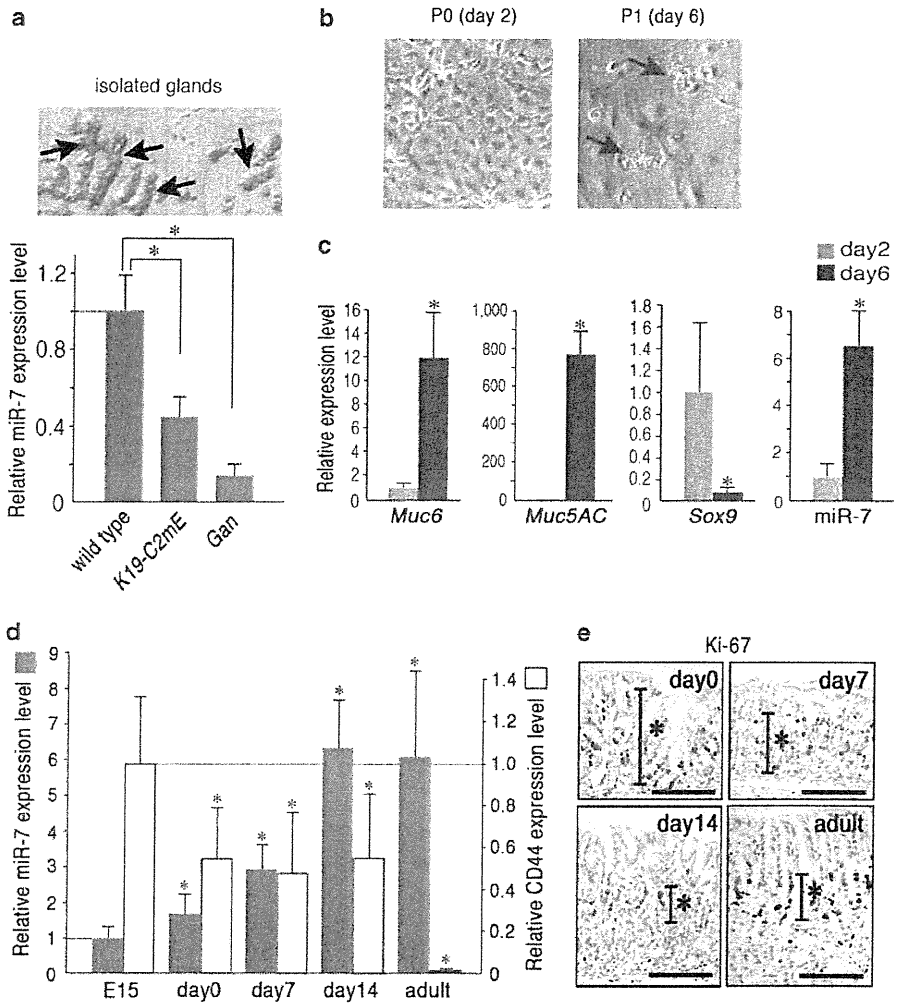

Figure 2 The induction of miR-7 expression in differentiated gastric epithelial cells. (**a**) A representative photograph of isolated gastric glands from wild-type mice (top, arrows). The expression levels of miR-7 in the isolated gastric glands of *K19-C2mE* and *Gan* mice relative to the wild-type level are shown (mean ± s.d.) (bottom). $*P<0.05$. (**b**) Representative photographs of primary cultured gastric epithelial cells on day 2 (passage 0: P0) and on day 6 (passage 1: P1) (original magnification, × 100). Arrows in P1 indicate mucin-containing enlarged cells on day 6. (**c**) The levels of *Muc6*, *Muc5AC* and *Sox9* mRNA and miR-7 in the primary cultured gastric epithelial cells on day 6 (closed bars) relative to the levels on day 2 (gray bars) are shown (mean ± s.d.). $*P<0.05$ versus the day 2 level. (**d**) The expression levels of miR-7 (gray bars) and *CD44* (open bars) in the stomach at the indicated ages relative to the levels in E15 embryos are shown (mean ± s.d.). $*P<0.05$ versus the E15 level. The expression levels of miR-7 were normalized to the Sno202 level. (**e**) Representative photographs of Ki-67 immunostaining in the glandular stomach of mice at the indicated ages. Asterisks indicate proliferative zones. Scale bars indicate 50 μm.

significantly decreased cell proliferation in both cell lines compared with control vector-transfected cells (Figure 3d). Moreover, pre-miR-7 transfection significantly suppressed soft agar colony formation in both cell lines (Figures 3e and f). These results strongly suggest that miR-7 has a tumor-suppressor role in gastric cancer development.

Repression of miR-7 in gastric cancer cells by macrophage-derived factor(s)

We detected primary (pri)-miR-7-1, pri-miR-7-2 and pri-miR-7b in the mouse normal stomach by real-time RT–PCR (Supplementary Figure 2), suggesting that mature miR-7 is processed from all these primary miR-7 in the normal gastric mucosa. MiR-7-1 is located in the intron of the *Hnrnpk* gene, and a CpG island is found in the promoter region of *Hnrnpk* (Supplementary Figure 3a). On the other hand, we could not determine CpG islands that regulate the transcription of miR-7-2 and miR-7b. We thus examined DNA methylation in the CpG islands in the *Hnrnpk* promoter region. Notably, DNA methylation levels in *K19-C2mE* gastritis and *Gan* mouse tumor tissues were not increased compared with the wild-type mouse stomach (Supplementary Figure 3a). Consistently, DNA methylation was not detected in the promoter region of the *HNRNPK* gene in human gastric cancer tissues (Figure 4a). We also examined the trimethylation of histone H3 at lysine 27 (H3K27me3) in